



The Role of Orosi's Islamic Geometric Patterns in the Building Façade Design for Improving Occupants' Daylight Performance

Seyedeh Nazli Hosseini,^a Seyed Morteza Hosseini,^{*b} Milad HeiraniPour^c

^a Department of Interior Architecture, Faculty of Architecture & Urban Planning, University of Art, Tehran, Iran

^b Smart Architectural Technologies, Department of the Built Environment, The Eindhoven University of Technology, The Netherlands

^c Department of Architecture and Energy, Faculty of Architecture & Urban Planning, University of Art, Tehran, Iran

Article info

Article history:

Received 15 September 2020

Revised 23 October 2020

Accepted 27 October 2020

Published online 7 November 2020

Keywords:

Building façade design

Occupants daylight performance

Islamic geometric patterns

Orosi

Abstract

The form of the building facade significantly affects the amount of useful daylight admitted in the interior space. Striking a balance between the visual comforts of occupants and taking advantage of daylight is always a challenge and, therefore, investigating complex, geometric forms of Orosi patterns can be an effective way of improving visual comfort alongside the aesthetic aspects. Due to intense radiation in the hot and arid climate of Iran, passive strategies were employed for controlling natural light. As a daylight-related component in Iranian vernacular architecture, Orosi offers different functions which are divided into three categories, namely daylight performance, thermal performance, and decorative role. In an attempt to improve indoor daylighting and visual comfort of occupants, this paper investigated, for the first time, the daylight performance of different Islamic geometric patterns (IGPs) used in Orosies with different thicknesses on the West and south facade. To this end, a total number of twelve traditional courtyard houses were studied through a field survey to extract different types of IGPs used in the Orosies. Finally, a grid-based simulation analyzed the indoor daylight conditions through climatic-luminance based metrics. The findings confirmed the daylight performance of the IGPs as a complex geometric form used for the facades. Compared to the base case on the South façade, all the studied patterns offered a significant potential to address the requirements of visual comforts. Additionally, the results revealed the considerable effect of thickness on the daylight performance of IGPs. Based on the results, the 10 and 15 cm thicknesses, showed better results, in comparison with the 5 cm thickness. The 8-Point-Star, as the best choice for the South façade, kept the metrics within an adequate range for occupants. The 8-Point-Star provided DA, UDI, EUDI, and sDA values of 80.18%, 76.65%, 12.22%, 44.6 respectively for thicknesses of 10 cm in the bright layer, which is more than twice the UDI value provided by the base model. Furthermore, the results confirmed the poor performance of IGPs on the West façade, particularly with thicknesses of 10 and 15 cm. The 8-Point-Star and 8-Fold-Rosette, as the best choices, improved the daylight performance of the West façade and prevented visual discomfort for occupants.

© 2020 The Author(s). Published by solarlits.com. This is an open access article under the CC BY license (<https://creativecommons.org/licenses/by/4.0/>).

1. Introduction

Natural light, as a renewable and permanent energy resource, is an influential factor in designing energy-efficient buildings, helping to significantly reduce the need for artificial lighting [1,2]. Moreover, distributing sunlight and diffusing it in the interior environment provides positive impacts on the physiological and psychological health of occupants [3–5]. Exploiting natural light during the daytime is a pivotal element in providing a desirable indoor space for occupants, which in turn results in higher

awareness, improved mood, less fatigue, and reduced eye strain [6,7]. Moreover, a well-daylight space is associated with the quality of visual comfort experienced by the occupants [3,8]. Considering that occupants spend a major portion of their time in interior spaces, either office or home, the provision of adequate daylight is one of the main objectives of architects and engineers in the early stage of designing residential buildings [9–11]. Architects have attempted to approach this goal from different perspectives, including changing the façade structure, occupants' behaviors, or supplying lighting resources according to residents' requirements. These approaches are mostly concerned with climatic conditions and dynamic characteristics [12–14]. Vernacular architecture benefits from various design strategies for

*Corresponding author.

S.Nazli.Hosseini@gmail.com (S. N. Hosseini)

s.m.hosseini@tue.nl (S. M. Hosseini)

archmiladheirani@gmail.com (M. HeiraniPour)

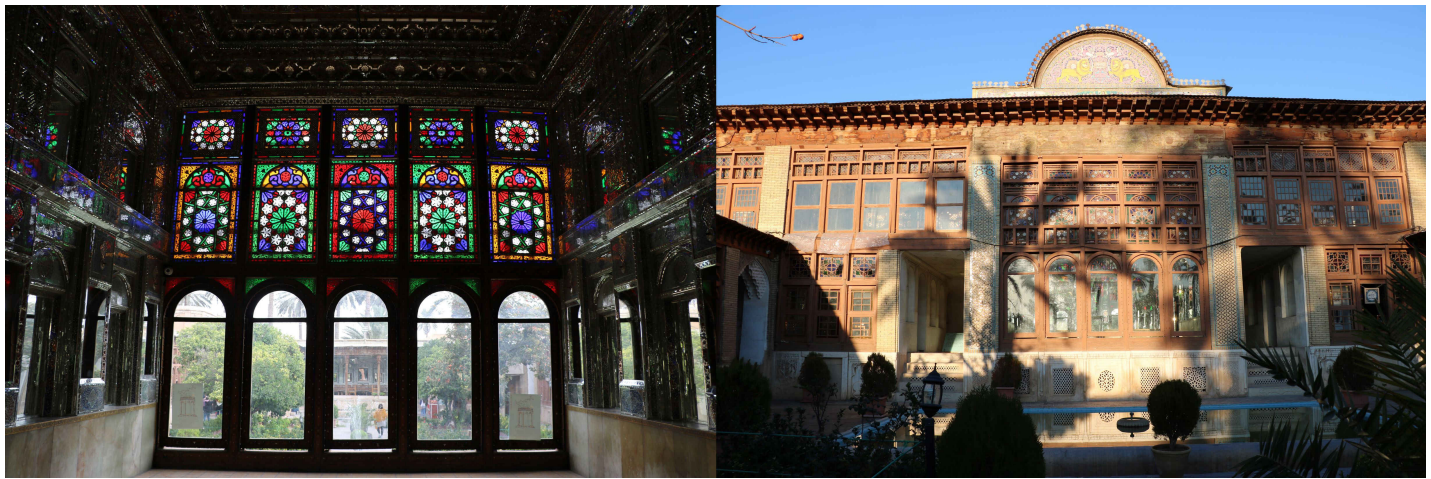


Fig. 1. Orosi of Zinat-Al-Molk house Shiraz, Iran.

providing occupants comfort conditions [15]. Thus, implementing its underlying principles into the design of buildings' façade facilitates achieving visual comfort and daylight performance for the occupants [16].

Iran, as one of the first ancient civilizations, has a rich traditional architecture. Despite the harsh climatic conditions, its architecture has provided a desirable internal environment [17,18]. Sunlight, as an important design factor, formed the fabric of cities and configuration of buildings. Due to intense radiation in the hot and arid climate of Iran, novel strategies have been employed for controlling and directing natural light [19]. In particular, Orosi window is a light controller in the traditional Persian houses generally considered in façades in different types of climates [20] (Fig. 1).

Orosies were categorically types of sash windows specifically built with aesthetic aspects in mind while admitting an adequate amount of daylight in the indoor space [21–23]. Orosi is the combination of wooden panels with Islamic Geometric patterns (IGP) and colorful glasses. The movable panels were opened by the vertical sliding movement, and were responsible for controlling the amount of light passing through, thus a qualified illumination. Moreover, Orosies were effective in satisfying the visual privacy requirements of occupants [24–26] (Fig. 2), and, therefore were frequently used at the central hall called Shahneshin, which was the official room for special ceremonies and important gatherings [27,28]. It should be noted that the Qajar period is known as the golden age and focal point of the construction and use of Orosi. Surprisingly, using modern construction method with steel structure gave rise to a dramatic decline in incorporating Orosi into buildings [29–38].

In brief, Orosi has been mentioned as a daylight-related component capable of perform different functions mainly divided into three categories: daylight performance, thermal performance, and decorative role.

Thermal performance: In addition to the Orosi's influence on daylight conditions, some studies have particularly attempted to assess thermal aspects of openings. Sharif et al. [39] performed a library study and field survey in the tropical and subtropical steppe climate to evaluate thermal role of Islamic Geometric patterns (IGP) of Orosies, called *Girih*. They believe that, from a theoretical perspective, applying *Girih* to architectural elements,

including openings along the western side might have climatic logic such as providing thermal comfort as well as natural ventilation [39].

Decoration role: Despite of the thermal and daylight performance of Orosies, many researchers have emphasized on their aesthetic aspects. Importantly, scholars have considered three, determining factors related to the aesthetic aspects, namely colorful glasses, patterns, and construction techniques. Holding a valuable position in Islam and religious beliefs, light has been an element highly emphasized by architects. For example, colorful glasses have been used to present various colorful views relying on the visual and spiritual manifestation of light [26,32–40]. In addition, since technical advancement has diversified the forms and compound IGP were used in Orosies, some researchers have studied the construction techniques from the perspective of aesthetics, color, and patterns. They have technically categorized these techniques to find the similarities and differences [41,42]. Reporting, patterns as an influential characteristic in the design

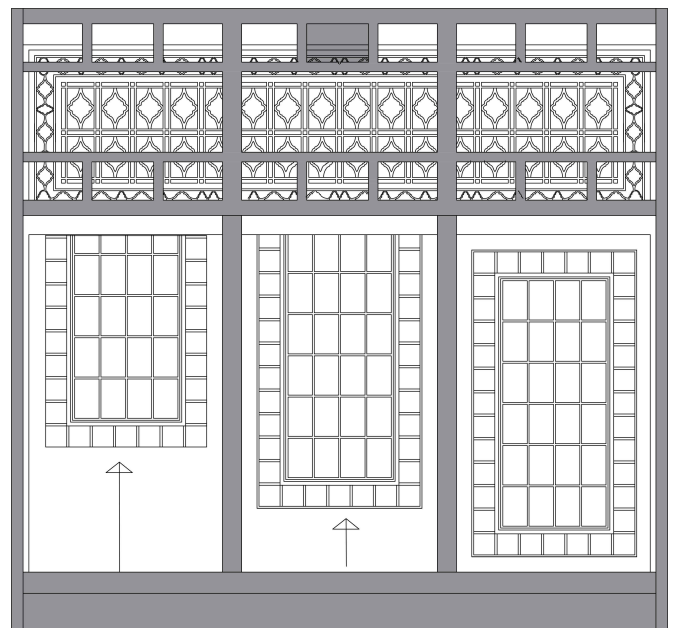


Fig. 2. Orosi, the vertical sliding movement controls the amount of passing light.

and construction techniques, studies have pointed out that in the beginning, simple patterns were often used shifting to more complex ones in later periods [30,43,44].

Table 1 briefly analyzes the researches on Orosi windows, based on research methodology, software, climate, building type, function, and effective architectural parameters:

- Most researchers have tried to study Orosies through library studies, field surveys, and case studies. Only a few have simulated the behaviors of the Orosies. Despite having both thermal and daylight behaviors, simulation tools were used just to assess daylight performance. Advanced daylight calculations have been carried out through different software packages, including Ecotech, Radiance, Diva, and Grasshopper plug-ins, such as Honeybee and Ladybug.
- Orosies have been investigated commonly in dry climate types (Group B), including hot desert climate (BWh), cold desert climate (BWk), and cold semi-arid climate (BSk).

- Most researchers have studied Orosies in vernacular buildings, whereas only one study exists to investigate Orosies in contemporary architecture. Conducting further research in this regard can lead us to find ways of using Orosies as an effective architectural element in contemporary buildings.
- Factors including geometry, WWR, dimensions, and color were considered as the most studied factors in daylight performance and decorative role. However, pattern was the least studied factor, particularly in terms of dealing with lighting.
- Thermal performance has only been assessed from a theoretical perspective rather than detailed analysis. Heat gains of Orosies have been relatively neglected and is by far the least developed aspect of Orosi windows.

In summary, several studies have worked on Orosi and its characteristics as an architectural element. Although, Hosseini

Table 1. Summary of Literature review.

Num.	Author	Year	Methodology	Software	Climate	Building Type	Function	Effective Parameters
1	Tahbaz et al [45]	2018	LS/CS/FS	-	BWh	V	DP	G/PD
2	Tahbaz et al [20]	2014	LS/SA/FS	R	BWh	V	DP	O/PD/WWR/M/C
3	Tahbaz et al [46]	2016	LS/FM/SA	R	BWh	V	DP	O/G
4	Tahbaz&Moosavi [4]	2009	LS/SA/FM/	-	-	V	DP	O/G/AG
5	KazemZade&Tahbaz [47]	2013	LS/SA/	E	BWk	V	DP	O/G/BF
6	Mousavi et al [48]	2019	LS/CS/NA	-	BWh	V	DP	G/PD/O/WWR
7	GorjiMahlabani&MofradBoushehri [33]	2017	LS/CS/LM	-	BSk	V	DP	C/O/G/ WWR
8	Nabavi et al [22]	2013	LS/CS	-	B	V	DP	BF/G
9	Khamechian et al [31]	2018	LS/FS/CS	-	BWh	V	DP	BF/PD/G
10	GorjiMahlabani&MofradBoushehri [33]	2017	LS/CS/FM	-	BSk	V	DP	C/AG
11	Haghshenas et al [34]	2016	LS/FS/LM/	-	BWh	V	DP	AG/C
12	Wahdattalab&Nikmaram [35]	2017	LS/CS/FS	-	BSk	V	DR	C/G/P
13	Hosseini et al [25]	2018	LS/SA	Rh/G/D	BWh	C	DP	G/O/WWR/C
14	Sharif et al [39]	2017	LS/CS/FS	-	BSk	V	TP	O/WWR
15	Makani et al [49]	2012	LS	-	B	V	DP / DR	BF/O/PD/C
16	Ayvazian [38]	2004	LS	-	-	V	DP / DR	PsE/ PhE
17	Boubekri [37]	2008	LS	-	-	V	DP / DR	PsE/ PhE
18	Vaafi [36]	2002	LS/CS	-	BSk	V	DP / DR	FB/PD/O
19	Madhoushiannezhad &Alamooti [42]	2016	LS/DA	-	BSk	V	DP	G/PD/WWR/M/C
20	Fathi&Farsani [28]	2014	LS/CS/FW	-	-	V	DR	P/ CT
21	Habib et al [26]	2013	LS/FS/CS	-	BWh	V	DP	-
22	Jalili&Nazari [41]	2016	LS/CS/DA	-	BWh	V	DP / DR	C/PsE
23	Abdullahi&Embi [43]	2013	LS/CS	-	-	V	DR	P/G
24	Marotta [44]	2018	LS/CS	-	-	V	DR	P/G
25	Faghihi et al [24]	2017	LS	-	-	V	DR	C/PsE/PhE
26	Javani [40]	2010	LS	-	-	V	DR	C/PsE/PhE
27	Hosseini et al [32]	2020	LS/SA	Rh/G/D	B	M	DP	C

Method: LS: Library Study, CS: Case Study, FS: Field Survey, SA: Simulation Analysis, LM: Laboratory Measurements, DA: Descriptive Analytics, NA: Numerical Analysis; **Software:** E: ECOTECH, Rh: Rhino, G: Grasshopper, D: Diva, R: Radiance; **Climate:** BWh: Hot Desert, BSk: Cold Semi-arid, BWk: Cold Desert, B: Arid and Semi-arid; **Building Type:** C: contemporary, V: Vernacular; **Function:** DP: Daylight Performance, DR: Decoration Role, TP: Thermal Performance; **Effective Architectural Elements:** G: Geometry, O: Orientation, AG: Albedo of Glass, M: Material, PD: Proportion and Dimension, BF: Building Form, WWR: Window-to-wall Ratio, C: Color, P: Pattern; **Other:** PsE: Psychological effects, PhE: Physiological Effects, CT: Construction Technique

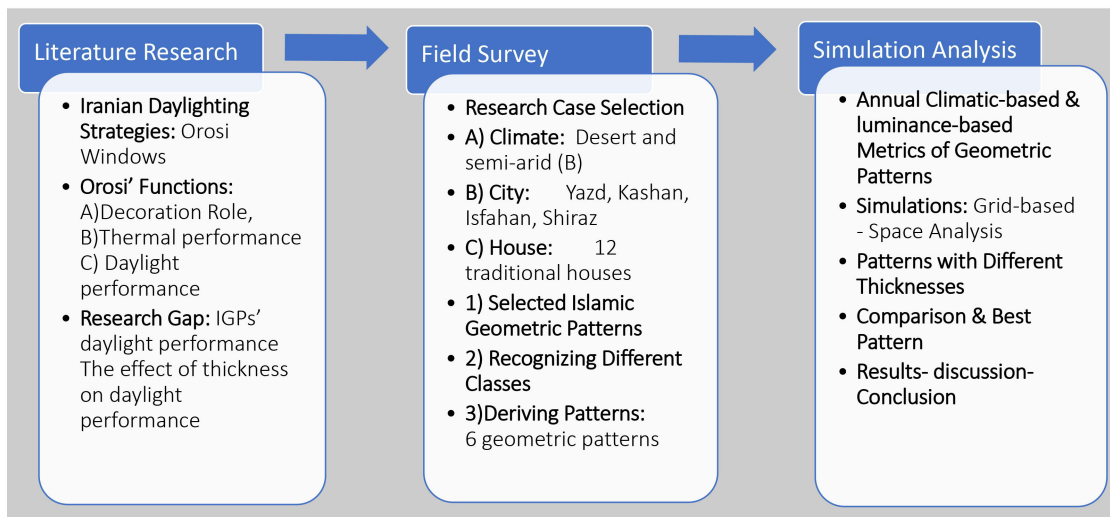


Fig. 3. Illustrating research process.

et.al [25] have mentioned the high potential of integration of colored glass and geometrical patterns in façade, no researchers have provided an in-depth study about the impact of Orosi patterns on daylight performance and visual comfort.

Given the lack of research in this area, this study mainly focused on IGPs in a region with desert and semi-arid climate. Harch solar radiation is a challenging problem for this group of climates and, therefore, the present study aims to bring IGPs to focus and try to answer the following research questions:

- Which IGPs have been employed in the Iranian Orosi windows?
- What is the IGPs' daylight performance?
- What is the difference between the different types of IGPs and how do they affect daylight performance and occupants' visual comfort?

How daylight performance is affected by the thickness of IGPs?

2. Research methodology

The present study investigates the daylight performance of Orosi patterns, through library study, a field survey and daylight simulation analysis (Fig. 3) as explained in the following.

2.1. Literature review

A literature review was carried out on the concept of Orosi and its characteristics, as one of the daylight strategies and architectural elements in Iranian traditional architecture (Table 1). In terms of search queries, a wide range of words and phrases, such as daylighting performance, vernacular architectural elements, Orosi and IGPs were considered to conduct a comprehensive literature analysis.

2.2. Filed survey

A field survey was also conducted using twelve traditional houses as the case studies, in order to identify the geometry, location of openings, and patterns in four cities located in the desert and semi-arid (B) climates. The Selection process of cases was conducted based on the following step:

- Climate selection:** Under the Köppen climate classification, four climatic zones were recognized in Iran [19]. However, this study focuses on the desert and semi-arid (B) climate as the main classification, which covers two-thirds of Iran. Furthermore, due to the intensity of radiation in this region, the most unique Orosies can be found.
- City selection:** Four ancient cities, namely Yazd, Kashan, Isfahan, and Shiraz are selected from this climate. These cities are well-known due to their long history and cultural heritage. Many monuments can be found in Kashan, ranging from the Sialk Hill to houses of the Qajar era, showing that this city has been a focus of Iranian history [19]. One of the oldest cities of ancient Persia is Shiraz, traced back to 2000 BC. It was the capital of Fars province during the Qajar era [50]. Meanwhile, Isfahan is another of the most ancient cities in Iran, with a strong history traced back to the 16th century according to the discoveries [51]. Regarding the last selected city, Yazd, the first mention in historic records predates it back to around 3000 years BC. It is still famous for its mud-brick and elegant courtyard houses [52].
- House selection:** Twelve traditional houses are selected for survey as case studies. These selected houses have been marked as valuable based on the study conducted by the Iran Cultural Heritage, Handicrafts, and Tourism Organization [53]. They were analyzed accordingly through different approaches, such as climate type, the geometry of windows, location of Orosi, and its type, and name of patterns.

2.3. Simulation analysis

Since Islamic and Iranian architecture broadly identifies itself with geometric design [54], four types of symmetry have aided to create noble patterns. The design process generally followed hierarchical levels labeled as motifs, compound motifs, and patterns. Daylight simulation was then performed through annual climate-based daylight metrics and luminance-based daylight metrics using spatial daylight autonomy (sDA), daylight autonomy (DA), useful daylight illuminance (UDI), exceed useful daylight illuminance (EUDI), and daylight glare probability (DGP). Finally, the overall performance of different patterns was compared through analysis

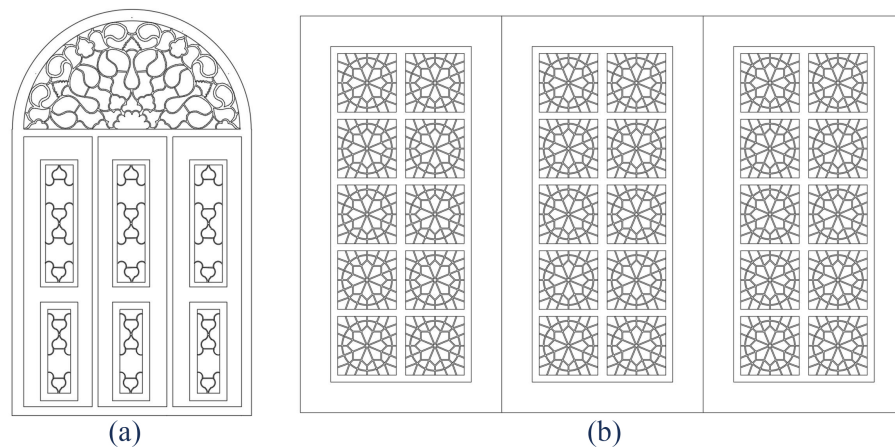


Fig. 4. General division of patterns: (a) floral pattern and (b) geometrical patterns.

and discussion. This allowed us to identify and assess the impact of different patterns on the quality of daylighting in spaces.

3. The design and construction of geometric patterns

3.1. Motif identification (morphology)

Islamic art and architecture are based on patterns that can be generally classified into two main categories of floral and geometrical ornaments (Fig. 4). The growth and spread of geometry through Islamic art and architecture are associated with the development of science and technology in the Middle East, Iran, and central Asia [54]. Consequently, this has resulted in the widespread use of geometric patterns. They were commonly driven from triangle, rectangle, and pentagon, which are known as the origin of Islamic art [43,55]. These decorative elements can be noticeable in different parts of a building, for instance, walls, windows, and doors [56]. Orosi, as a kind of window and luxurious decoration, was constructed with different types of patterns [27]. Orosies were commonly used in houses in the different spaces ranging from bedrooms to the central Halls, (also called Shahneshtin) [24]. Since these patterns can affect indoor conditions, the current research has studied several traditional houses in the different cities of Iran. The set of basic motifs was daylight identified as the cases for daylight performance simulation.

Table 2 briefly represents the structure and composition of the patterns used in the case studies based on the following factors: location, city, and their climate types. Hence, the classification of patterns was identified and eventually, the name of patterns was reported. A summary concluded from Table 2 is presented as follows:

- Orosies have been investigated in two climate types, namely hot desert (BWh) and cold desert (BSk).
- Orosies have been observed in different building orientations. It seems there was no obvious relation between their locations. A comprehensive investigation is required for traditional courtyard buildings.
- The geometry of windows can be divided into two categories, namely the rectangular and arched shapes which were related to the construction technique.
- The patterns are divided into two types: geometric and floral patterns. It seems geometric patterns has the largest share, which might be related to the construction techniques.

- Simple grid have been found at the lowest part of the window, which might be due to admission of adequate indoor daylight.
- Geometrical patterns, including 10-fold-Rosette (Fig. 6(d)), 8-point star (Fig. 6(c)), octagon (Fig. 6(b)), 8-fold-Rosette (Fig. 6(e)), and 6-point star (Fig. 6(a)) have been widely used in Orosies.

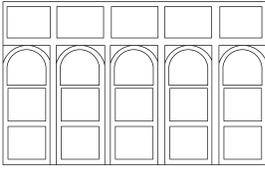
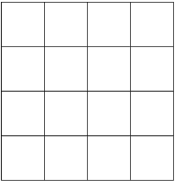
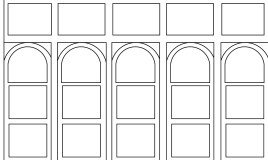
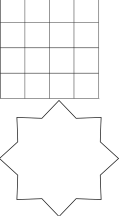
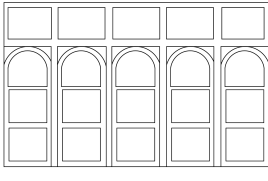
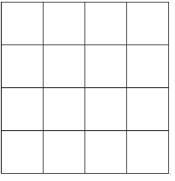
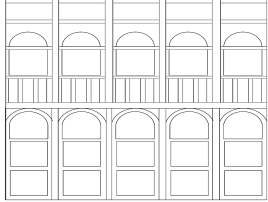
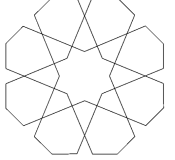
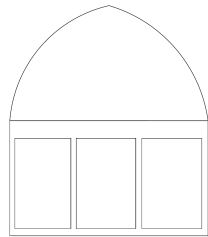
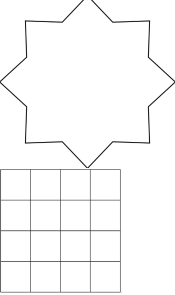
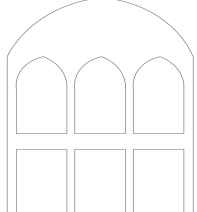
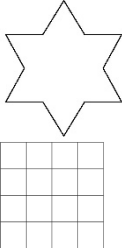
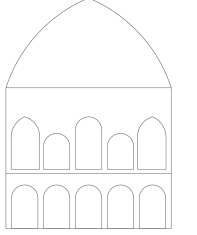
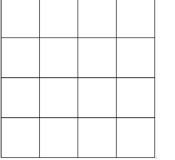
Based on Table 2, Orosi was used in different climate types, including BWh and BSk, which may be due to the necessity of harvesting daylight during day time. However, no clear relationship has been found between climate type and location of Orosi. Moreover, the Orosi window is well-known for its patterns, which are divided into two groups of geometric and floral depending on the construction techniques. Furthermore, various types of patterns as well as simple grids were employed in the Orosies. Generally, this study evaluated the daylight effectiveness and potential performance of geometric patterns in the desert and semi-arid climate.

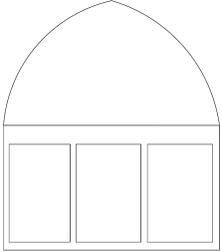
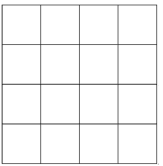
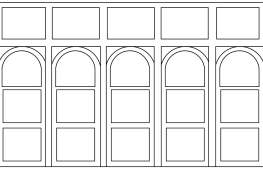
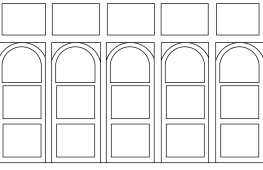
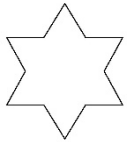
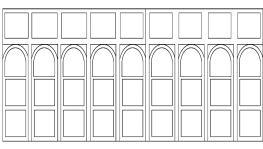
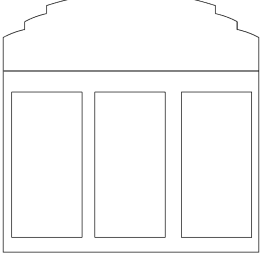
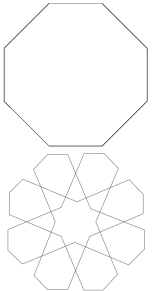
3.2. Daylight performance evaluation through climate-based metrics and luminance-based metric

Daylight performance of the facades was studied through climate-based metrics, including Daylight Autonomy (DA), Useful Daylight Illuminance (UDI), Exceeded Useful Daylight Illuminance (EUDI) and luminance-based metric including Daylight Glare Probability (DGP) [60]. sDA is defined as “the percentage of the occupied hours of the year when a minimum illuminance threshold is met by daylight alone” and for a point to be considered ‘daylit,’ the sDA at the point has to be 50%, in short sDA300 lx [50%] [60]. DA is defined as “the percentage of the occupied hours of the year when a minimum illuminance threshold is met by daylight alone” [61]. UDI is defined when “there is useful daylight in the back two-thirds of the space (UDI 100-2000 lx), while EUDI (UDI > 3000 lx) flags on over-supply of daylight near the façade” [60,61]. Glare is a human sensation, defined by Harper Collins as, “describes light within the field of vision that is brighter than brightness which the eyes are adapted [61]”. The well-known metric suggested by Wienold and Christofersen [62] is Daylight Glare Probability, which uses “CCD Camera based luminance mapping technology.” Furthermore, DGP has been categorized into four groups comprising imperceptible (30-35),

perceptible (35-40), disturbing (40-45) and intolerable (45-100) [61].

Table 2. The structure of all basic patterns and composition of case studies' patterns.

Name of House	City/ Climate	Location of Orosi	Geometry of Window		Pattern		
			Photo	Section	Classification	Name	Figure
Pakaryi	Shiraz/ BSk	W			G	SG	
Manteghinezhad	Shiraz/ BSk	S/N			G	SG/ 8PS	
Forough-Al-Molk	Shiraz/ BSk	W/S/N/E			G	SG	
Zinat-Al-Molk	Shiraz/ BSk	W/S/N/E			G	10FR	
KarimKhani [57]	Shiraz/ BSk	S/N/E			G	8PS/ SG	
Abbasian	Kashan/ BWh	S/N/E			G	6PS/ SG	
Manuchehri	Kashan/ BWh	S/E			G	SG	

Gilanian [58]	Isfahan/ Bwk	N			C	VM/ SG	
Mashroute	Isfahan/ Bwk	E			C	VM	-
Motamedi (Mollabashi)	Isfahan/ Bwk	N/E			C/G	VM/ 6PS	
Moshir-Al-Molk	Isfahan/ Bwk	S			C	VM	-
Lariha [59]	Yazd/ BWh	W/S/N/E			G	O/8FR	

Location of Orosi: *W*: West, *E*: East, *S*: South, *N*: North; **Climate:** *BWh*: Hot Desert, *BWk*: Cold Desert; **Classification of Patterns:** *C*: Curved, *G*: Geometric; **Name of Pattern:** *SG*: Simple Grid, *10FR*: 10-Fold Rosette, *8PS*: 8-Point Star, *O*: Octagon, *8FR*: 8-Fold Rosette, *6PS*: 6-Point Star, *VM*: Vegetation Motifs

3.2.1. Daylight performance simulation of islamic geometric patterns

The simulation is performed using Rhinoceros®, Grasshopper, and Diva for analyzing daylighting and energy modeling. DIVA simulation tools under Iran sky have been used in different studies by [1,25,32]. The simulation is made assuming that the office building is located in Yazd, Iran. The latitude of Yazd is 31.89, and the longitude is 54.35. Yazd has been classified under hot desert climate (BWh), which has clear sky based on the Koppen climate classification [63]. Furthermore, Yazd weather data used for the simulation process are available from the EnergyPlus website and arranged by the World Meteorological Organization region and Country [64]. Due to the privacy and lighting concerns, Iranian traditional buildings follow a hierarchy arrangement, resulting in the division of interior space into three layers: vicinity of façade (bright layer), intermediate space (semi-dark layer) and private space (dark layer) [22,64]. Therefore, simulation is performed based on these layers (Fig. 5). Iranian golden rectangle is applied for the test room plan drawn in a hexagonal [22], which

is based on a common method used in planning of rooms and courtyard in the Iranian traditional architecture. Thus, the width and depth of the floor plan were respectively 4.2 m and 7 m. Building elements are modeled with a thickness of 0.2 m for walls, and 0.3 m for ceiling and floor (Fig. 5 and Table 3). The height of the room from the top of the floor to the bottom of the ceiling is 2.8 m. Moreover, the window is located on the South and West façade with a ratio of 0.85 for the window to wall (Fig. 5). Climate based metrics including Daylight Autonomy (DA), Useful Daylight Illuminance (UDI), Exceeded Useful Daylight Illuminance (EUDI) are calculated annually for each façade configuration. Daylight Glare Probability (DGP) is the metric to evaluate luminance, which is calculated based on the different Islamic geometric patterns on the solstice and equinox days, namely December 21st, March 21st and June 21st [61]. In the present research, daylight glare probability has been calculated at the point, located in the center of the room, at a 2 m distance far from the window. The following assumptions are applied to the daylight performance simulation: clear sky with sun, minimum of 500 Lux on the work plane at a height of 0.85 m from the floor,

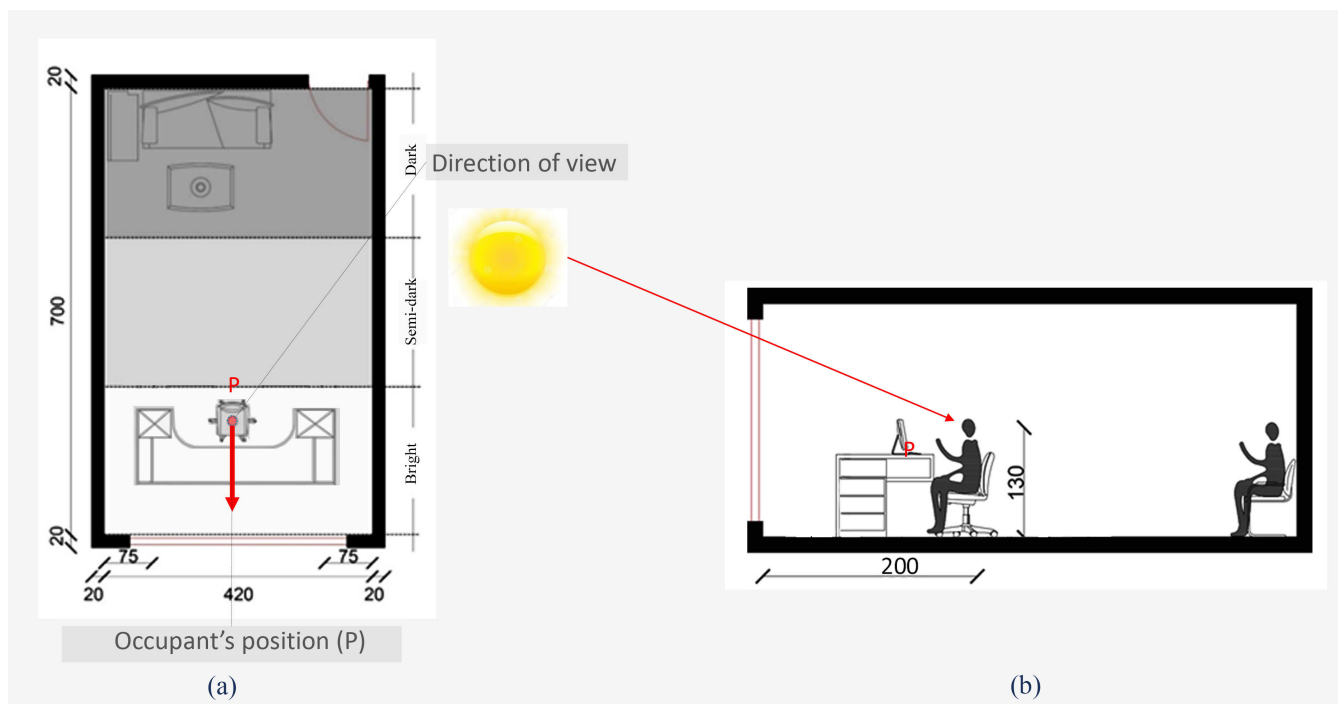


Fig. 5. (a) and (b) Division of reference room into three layers based on the hierarchy arrangement in Iranian vernacular architecture [34].

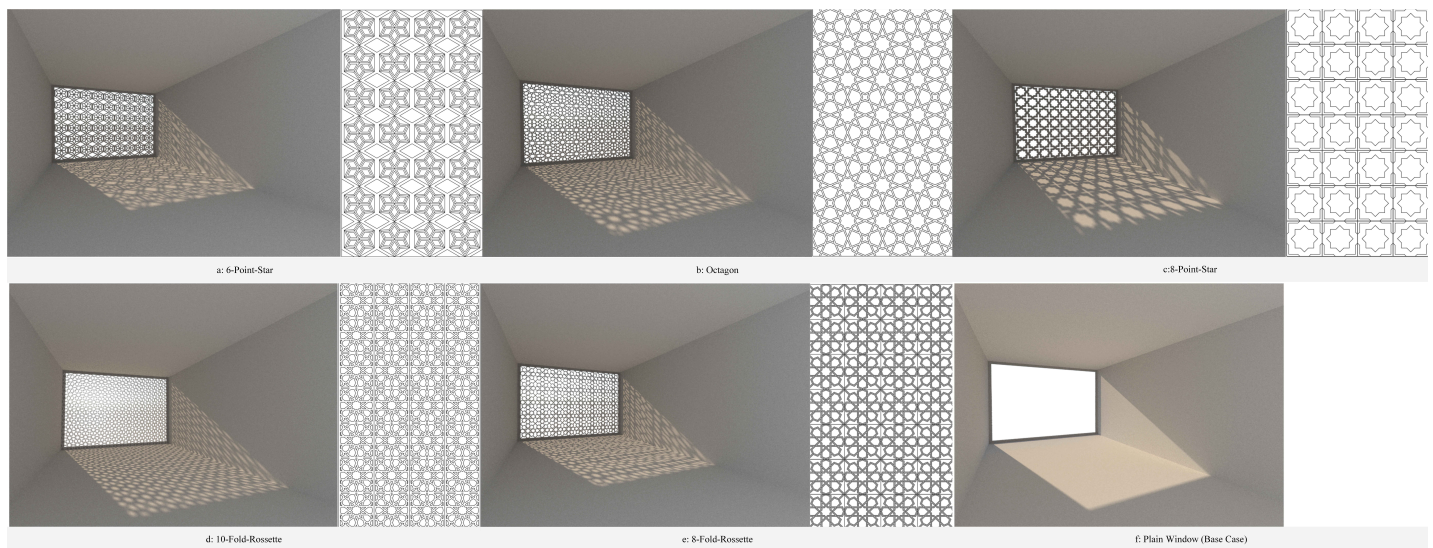


Fig. 6. The IGPs used in the simulations.

occupancy schedule (9:00, 12:00, and 15:00), a grid of sensors with lengths of 0.5 m in Y and X directions, no shading and artificial light [61].

3.3. Selected pattern

The patterns were driven and inspired by Orosi as the vernacular light catchers. These patterns are successfully able to block solar radiation and minimize glare issues. The patterns transmit an adequate amount of direct sunlight into the indoor environment. By diffusing light, they provide more visual comforts to the users. The structure of the composition and design of all the basic patterns used in the research study are presented by Table 2. The visual effect of composed patterns on shadow and direct solar radiation are represented in (Fig. 6).

4. Results and findings

The daylighting of an example office interior was investigated through numerical analysis of six case studies, namely 6-Point-Star (Fig. 6(a)), Octagon (Fig. 6(b)), 8-Point-Star (Fig. 6(c)), 10-Fold-Rosette (Fig. 6(d)), 8-Fold-Rosette (Fig. 6(e)), plain window (base model) (Fig. 6(f)). Tables 4–6 provide information about the indexes DA, UDI, EUDI, sDA, and DGP of the IGPs with three thicknesses of 5, 10, and 10 cm on the South façade.

The results suggest a complete visual discomfort for the plain window, as the base-case of the simulation. The Daylight Autonomy (DA) shows that although the rate of daylight entering the interior space is high, it diminishes as we approach farther from the façade. The highest DA values occur in the vicinity of the

Table 3. Optical Properties of Common Material Surfaces [58].

Material surface	Optical information
Interior floor	20% Diffuse reflectance
Interior wall	50% diffuse reflectance
Interior ceiling	80% diffuse reflectance
Single glazing	90% direct visual transmittance
Exterior building surfaces	35% diffuse reflectance
Exterior ground	20% diffuse reflectance

window at the rate of 89.25% (South façade) and 99.56% (West façade). The intermediate layers, show the value of 72.30% (South façade) and 99.78% (West façade). Also, DA of 75.65% (South façade), and 75.67% (West façade) occur in the dark layer. Based on the DAs values it is clear that illuminance is above the acceptable level in all three layers. The UDI values of 31.96%, 64.65%, and 68.78% (South façade), and 57.24%, 88.06% and 97.37% (West façade) for the bright, semi-dark, and dark layer respectively indicate that most of the daylight allowed in by the plain window is not useful resulting in visual discomfort for the occupants. Besides, the Exceed UDI of 60.28% and, 23.00% respectively in the bright and semi-dark layers of South façade and the EUDI of 42.78% for West facade are suggestive of oversupply of daylight, causing occupants thermal discomfort and unwanted solar gain. Moreover, concerning the prediction risk of glare,

simulations have been performed based on occupants and sun positions at three different times of the solstice and equinox days. The results, with an average of 0.78, 0.71, and 1.00 for the South façade and also 0.54, 0.53, and 0.41 for the West facade (respectively on 21st March, June and December) prove intense visual discomfort for the base case (Figs. 7-9).

4.1. Annual climate-based metrics and luminance-based metrics of geometric patterns on the south façade

4.1.1. Climate-based metrics evaluation for cases with thickness of 5 cm

The simulation results confirmed the high performance of the geometric patterns in the façade in improving daylight performance and visual comfort. Table 4 shows that the employed IGPs reduce the DA values in all three layers. In this case, the maximum reduction was achieved by Octagon (Fig. 6(b)), amounting to 56% in the dark layer, 45.10% in the semi-dark, and 72.75% in the bright layer. Although the DA was enhanced to a satisfactory level, the results point to a significant improvement of UDI in all layers. For instance, the UDI was increased in the bright layer up to 81.28% by Octagon (Fig. 6(b)), which is more than twice compared to that for the base model (31.96%) (Fig. 6(f)). Slight changes can be reported in the semi-dark and dark layers. Besides, comparing the EUDI value in the base model and the models employed IGPs is indicative of a significant decrease in

Table 4. Annual daylight simulation through climatic-based metrics evaluation for South façade with thickness of 5 cm.

Islamic Geometric Patterns	Daylight Autonomy			Useful Daylight illuminance			Exceeded Useful Daylight illuminance			sDA
	Bright	Semi-dark	Dark	Bright	Semi-dark	Dark	Bright	Semi-dark	Dark	
Base Model	89.25	72.3	57.65	31.96	64.65	68.75	60.18	23	0	100
8-Fold-Rossette	82.12	67.9	27.12	72	75.63	73.95	15.88	2.1	0	66.1
10-Fold-Rossette	74.93	28.62	2,55	81.18	80.15	66.72	8.88	2.03	0	33
Octagon	72.75	27.2	1.65	81.28	78.1	61.78	6.84	1.2	0	33
8-Point-Star	80.43	56.75	11.47	63.12	72.8	66.65	24.97	0.78	0	56.2
6-Point-Star	77.65	43.70	3.87	79.37	78.07	70.67	10.19	1.45	0	45.5

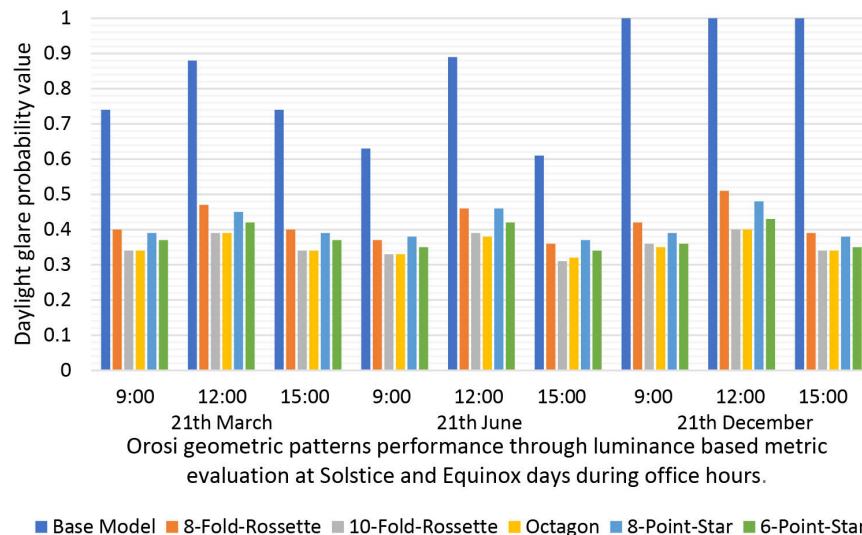
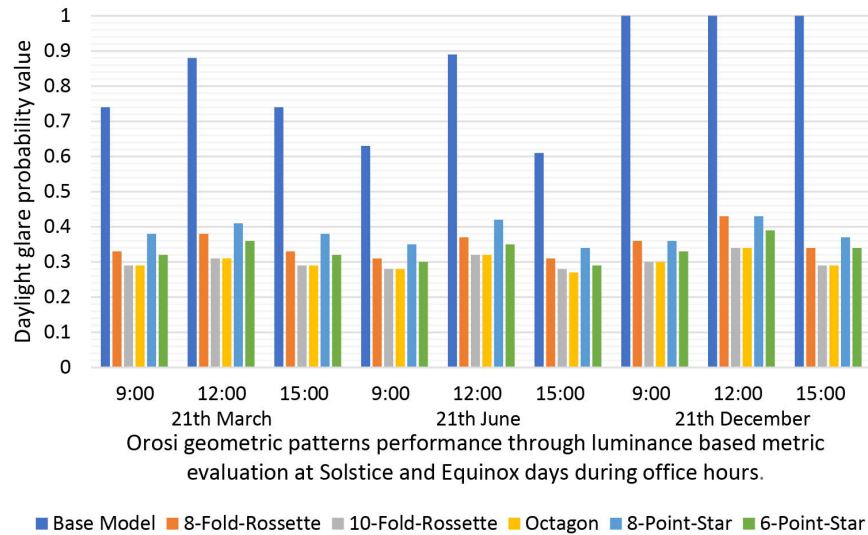


Fig. 7. Daylight glare probability of Orosi geometric patterns with thickness of 5 cm at Solstice and Equinox days during office hours.

Table 5. Annual daylight simulation through Climatic-based metrics evaluation for South façade with thickness of 10 cm.

Islamic geometric patterns	Daylight autonomy			Useful daylight illuminance			Exceeded useful daylight illuminance			Sda
	Bright	Semi-dark	Dark	Bright	Semi-dark	Dark	Bright	Semi-dark	Dark	
Base Model	89.25	72.3	57.65	31.96	64.65	68.75	60.18	23	0	100
8-Fold-Rosette	67.93	27.15	6.47	85.18	82.15	73.37	3.68	0.43	0	30.4
10-Fold-Rosette	30.46	1.3	0	81.81	41.7	13.37	2	0.3	0	8
Octagon	27.12	0.57	0	75.5	35.68	13.5	1.94	0	0	7.1
8-Point-Star	80.18	43.87	6.12	76.65	77.52	67	12.22	1.42	0	44.6
6-Point-Star	58.71	12.7	0.5	84.09	67.85	37.15	3.15	0.65	0	22.3

**Fig. 8.** Daylight glare probability of Orosi geometric patterns with thickness of 10 cm at Solstice and Equinox days during office hours.

this factor. The maximum reduction in EUDI occurred in the bright layer, experiencing a decrease from 60.18% to 6.84% (base model (Fig. 6(f)), Octagon (Fig. 6(b)) respectively). The semi-dark layer experienced smaller changes from 23.00% in the base model (Fig. 6(f)) to 1.45 % in the 6-Point-Star (Fig. 6(a)). Furthermore, to predict the risk of glare, a total of 54 simulations was conducted in three different times of the day as shown in Fig. 7. Despite the decrease in the DGP values compared to the base case, most of the results for the considered IGPs were within the imperceptible and intolerable glare range. The values revealed that problems are mostly associated with the semi-dark layer. Overall, despite decreasing the value of the DA, UDI, and EUDI, the 5 cm configuration is a poor choice to fulfill the DPG requirements.

4.1.2. Climate-based metrics evaluation for cases with thickness of 10 cm

Table 5 gives information about the effects of using IGPs in the façade as a functional element which can improve the indoor daylighting conditions. The results confirmed that increasing the thickness results in satisfying the visual comfort criteria. In terms of DA, pattern with a thickness of 10cm decreased this factor in bright and semi-dark layers up to 27.12% and 0.57% using Octagon (Fig. 6(b)), which is a considerable reduction in comparison with that of the base model (Fig. 6(f)) and models with a thickness of 5cm. In contrast, the UDI value was considerably increased pointing to a remarkable correction. T. The maximum

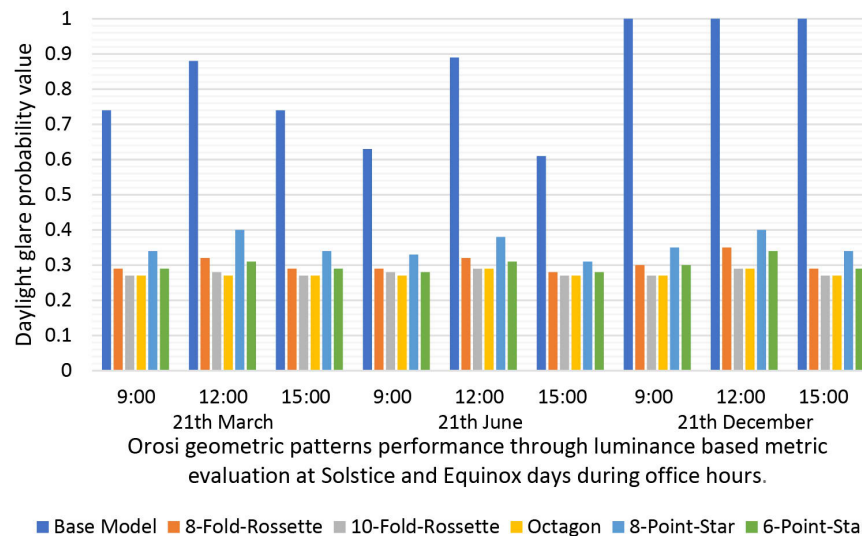
UDI has been brought to the rate of 84.09% in the bright layer, 82.15% in the semi-dark layer, and 74.37% in the dark layer by 6-Point-Star (Fig. 6(a)) and 8-Fold-Rosette (Fig. 6(e)). Moreover, comparing Exceed UDI value for plain window and IGPs showed a significant decrease from 60.18% to 1.94% in the semi-dark layer and from 23.00% to 0.00% in the dark layer using the Octagon (Fig. 6(b)). Moreover, the bar chart (Fig. 8) illustrates the results of DGP simulations for a total of 54 conducted simulations in three different times of the day, confirming an improvement in all values. They all remain in imperceptible and perceptible range except for the time 12.00 in all three days, at which time the 8-Point-Star (Fig. 6(c)) and 8-Fold-Rosette (Fig. 6(e)) are found within the distributing range.

4.1.3. Climate-based metrics evaluation for patterns with thickness of 15 cm

The findings support the effective role of the employed IGPs in the façade in improving visual comfort. Table 6 gives information about the changes in the DA with thickness of 15 cm. This parameter was decreased in the bright layer (5.46%), which is the lowest value in comparison with base case (Fig. 6(f)) and thicknesses of 5 and 10 cm. The semi-dark and dark layer experienced the values of 0.00% by the 10-Fold-Rosette (Fig. 6(d)) and Octagon (Fig. 6(b)) In contrast, the 8-Point-Star (Fig. 6(c)) brings about the DA of 71.00% in the bright layer. Moreover, the IGPs significantly increased the amount of UDI. For example, the

Table 6. Annual daylight simulation through Climatic-based metrics evaluation for South façade with thickness of 15 cm.

Islamic geometric patterns	Daylight autonomy			Useful daylight illuminance			Exceeded useful daylight illuminance			sDA
	Bright	Semi-dark	Dark	Bright	Semi-dark	Dark	Bright	Semi-dark	Dark	
Base Model	89.25	72.3	57.65	31.96	64.65	68.75	60.18	23	0	100
8-Fold-Rosette	13.84	1	0.17	69.09	43.45	33.47	1.94	0.15	0	0
10-Fold-Rosette	5.46	0	0	43.06	2.68	1	1.72	0	0	0
Octagon	5.75	0	0	46.03	1.4	0.775	1.72	0	0	0
8-Point-Star	71.00	21.40	1.87	83.75	76.8	56.75	5.81	0.6	0	29.5
6-Point-Star	58.71	12.7	0.5	64.47	21.75	9.9	1.9	0.05	0	22.3

**Fig. 9.** Daylight glare probability of Orosi geometric patterns with thickness of 15 cm at Solstice and Equinox days during office hours.

values of 64.47% in bright layer and 76.80% in the semi-dark layer (by 6-Point-Star (Fig. 6(a)) and 8-Point-Star (Fig. 6(c))) confirm the performance of IGPs in correcting UDI. However, in the dark layer, all the patterns showed poor performance compared to the base model (Fig. 6(f)). The EUDI was improved significantly by the 10-Fold-Rosette (Fig. 6(d)) and Octagon (1.72%) (Fig. 6(b)) in the bright layer. In the semi-dark and dark layers, the EUDI value is 0.00%. Besides, the DGP values from the bar chart of 54 simulations (Fig. 9) reveals that all the IGPs' simulations are within the imperceptible and perceptible range. The exceptions are observed only at 12:00 on 21st March and 21st December. The 8-Point-Star (Fig. 6(c)) brings a value of 0.40 %, causing disturbing glare.

4.1.4. Differences between cases with thickness of 10 cm and 15 cm

The findings confirmed the better daylight performance of the 10 and 15 cm thicknesses in meeting visual comfort criteria. In most of the simulations, the indices were observed within the appropriate ranges (Tables 4–6 and Figs. 7–9). The main differences between these two groups are pointed out in the following.

Thickness of 10 cm (Tables A.1 and A.2):

The Octagon (Fig. 6(b)) and 10-Fold-Rosette (Fig. 6(d)) caused the minimum of DA in all three layers. In terms of UDI, their

performances were not as expected, particularly in the semi-dark, and dark layers. In addition, both achieved the lowest EUDI values as well as the lowest DGP rates. Overall, with regards to the sDA value (7.10%, and 8.00% respectively) the Octagon and 10-Fold-Rosette could not meet the expectations for daylighting metrics to be within the adequate range.

The 6-Point-Star (Fig. 6(a)), as the next pattern, caused a significant decrease in the DA value and provided a high UDI value. The maximum UDI occurred in the bright layer (84.09 %). Additionally, the high percentages of UDI in the semi-dark and dark layers, (67.85%, 37.15% respectively), confirmed the high daylight performance. The EUDI experienced a considerable reduction in the bright and semi-dark layers (3.15%, 0.65% respectively). Furthermore, the DGP values were found in the imperceptible and perceptible ranges in all the situations. Overall, with regards to the sDA value (22.30%), the 6-Point-Star could not meet the expectations for daylighting metrics to be within the adequate range.

The next pattern, 8-Fold-Rosette (Fig. 6(e)), decreased the DA value and provided high rates of UDI. The highest UDI was 85.18%, and 82.15%, recorded respectively in the bright and semi-dark layers. Additionally, the low value of EUDI in the bright (3.68 %) and semi-dark layers (0.43 %), was suggestive of an efficient performance. Overall, with regards to the sDA value (30.40%), the 8-Fold-Rosette could not meet the expectations for daylighting metrics to be within the adequate range as well.

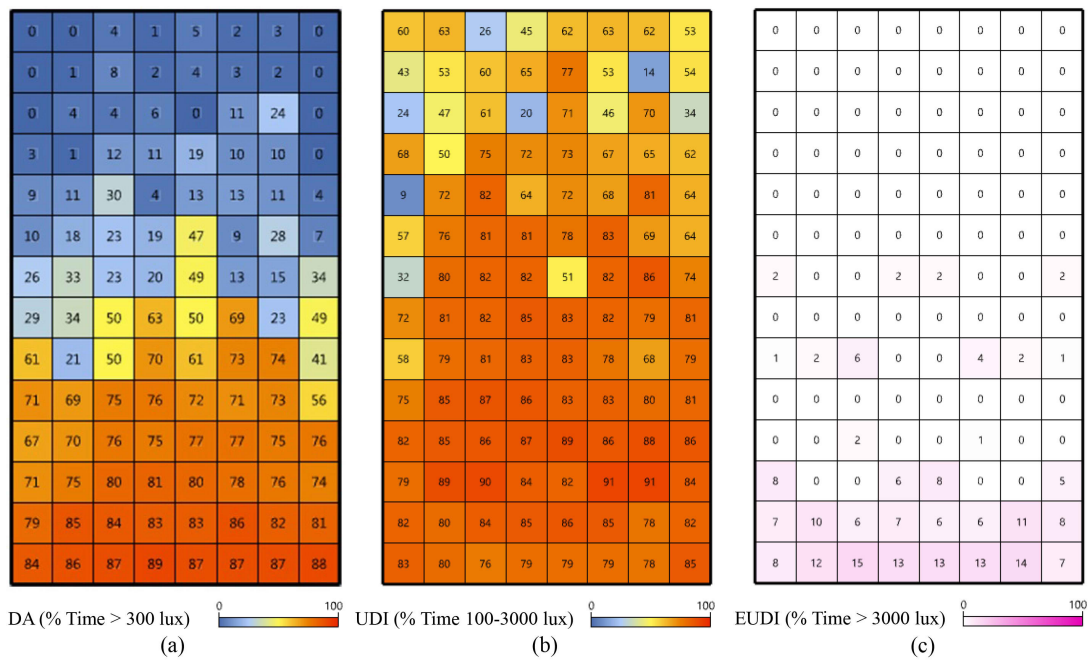


Fig. 10. Climate based daylight metrics grid evaluation (annual simulation) of 8-Point-Star for south facade (Fig. 5(c)). (a) Daylight Autonomy, (b) Useful Daylight illuminance, and (c) exceed useful daylight illuminance.

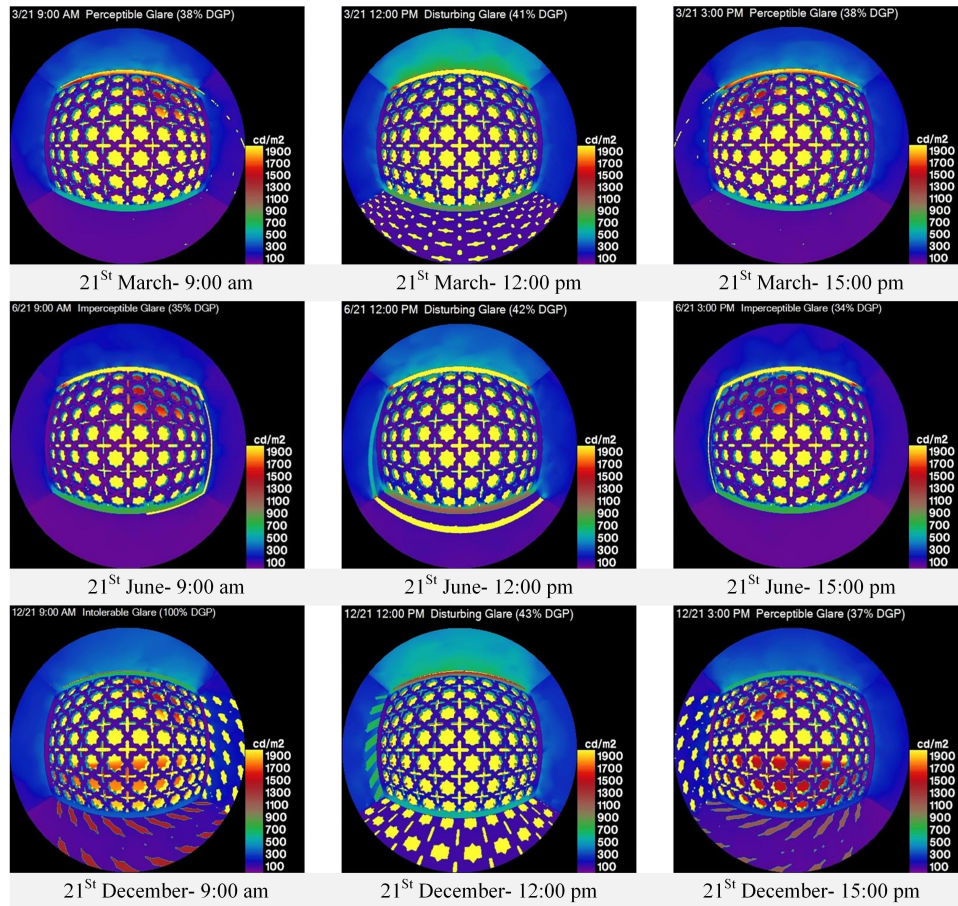


Fig. 11. Daylight Glare Probability (DGP) in three different days of 8-Point-Star for south facade (Fig. 5(c)).

The 8-Point-Star (Fig. 6(c)), as the last pattern, provided a higher DA, especially in the bright and semi-dark layers. Additionally, it achieved high UDI values, namely at rates of 76.65%, 77.52%, and 67.00%, (in the bright, semi-dark, and dark layers respectively). Moreover, the significant reduction of EUDI in the bright and semi-dark layers, (12.22%, and 1.42%

respectively), pointed out an effective performance. Furthermore, the reduced DGP met the requirements and was within the imperceptible and the perceptible range. As an exception, an undesirable value was reported, at the noon time of all the days. Overall, with regards to the sDA value (44.60%), the 8-Point-Star can, under particular conditions, meet the expectations for providing daylighting metrics to be within at the adequate range.

Thickness of 15 cm (Tables A.3 and A.4):

Applying the Octagon (Fig. 6(b)) and 10-Fold-Rosette (Fig. 6(d)) resulted in the lowest DA in all three layers while offering a low EUDI percentages in all three layers. Moreover, the Octagon achieved the lowest DGP, followed by 10-Fold-Rosette. Overall, with regards to the sDA value (0.00%), which is the lowest rate among the other patterns, the Octagon and 10-Fold-Rosette could not meet the expectations for daylighting metrics to be within the adequate range.

The 8-Fold-Rosette (Fig. 6(e)) resulted a significant reduction in the DA value, which was reported at the rates of 13.84%, 1.00%, and 0.17% (the bright, semi-dark, and dark layers, respectively). Moreover, this pattern provided a high UDI in the bright layer (69.09 %), whereas, the semi-dark and dark layers experienced a lower amount of UDI. The findings also confirmed the effective impacts on DPG values. It was reduced up to the imperceptible and perceptible range (0.28% - 0.35%). Overall, with regards to the sDA value (0.00%), the 8-Fold-Rosette could not meet the

expectations for daylighting metrics to be within the adequate range.

The 6-Point-Star (Fig. 6(a)), proved to be efficient and provided a DA value at the rate of 58.71% (bright layer). Moreover, a high UDI was obtained, particularly in the bright layer 64.47%). A substantial reduction in the EUDI values was observed, especially in the bright layer (1.90%). Affecting the DGP values resulted in the imperceptible glare to range from 0.28% to 0.34%. Overall, with regards to the sDA value (22.30%), the 6-Point-Star could not meet the expectations for daylighting to be within the adequate range.

The 8-Point-Star (Fig. 6(c)), as the last case, offered a higher DA, particularly in the bright layer (71.00%) as well as a considerable increase in the UDI values. It enhanced daylight conditions by providing UDI values at the rates of 83.75%, 76.80%, and 56.75%, (bright and semi-dark, and dark layers, respectively). Moreover, the low EUDI in the bright and semi-dark layers highlighted the effective role of the pattern. Furthermore, the DGP was reduced within the imperceptible and perceptible range. Exceptionally, results reported disturbing DGP at the rate of 0.40% at the noon time on the 21st March and 21st December. Overall, with regards to the sDA value (29.50%), the 8-Point-Star was able to meet the expectations for daylighting metrics to be within the adequate range (Figs. 10 and 11).

Table 7. Annual daylight simulation through Climatic-based metrics evaluation for West façade with thickness of 5 cm.

Daylight autonomy			Useful daylight illuminance			Exceeded useful daylight illuminance			sDA
Bright	Semi-dark	Dark	Bright	Semi-dark	Dark	Bright	Semi-dark	Dark	
89.25	72.3	57.65	31.96	64.65	68.75	60.18	23	0	100
94.28	57.75	21.1	87.32	93.24	86.74	12.21	3.75	0.07	45.15
61.43	26.21	3.97	88.24	74.10	28.72	8.81	3.06	0.10	25.96
62.21	23.84	3	88.64	72.57	24.82	8.03	2.15	0.05	25
97.03	56.65	17.17	82.04	91.71	71.35	17.87	5.03	0.50	46.15
76.71	39.43	8.37	87.59	88.25	42.12	10.56	3.71	0.40	34.62

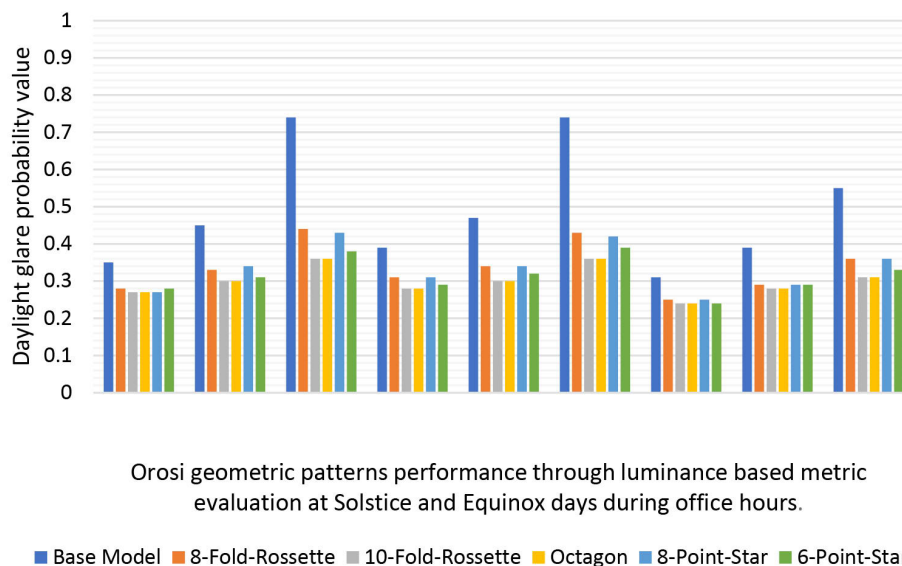
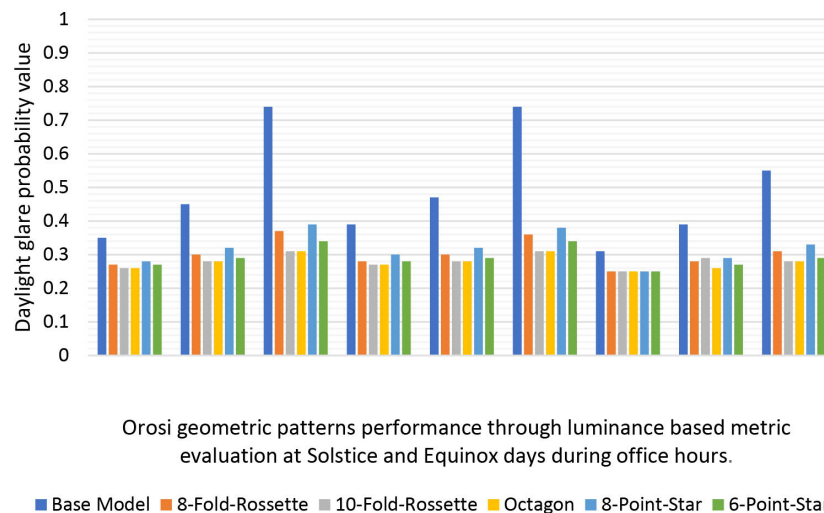


Fig. 12. Daylight glare probability of Orosi geometric patterns with thickness of 5 cm at Solstice and Equinox days during office hours, West Façade.

Table 8. Annual daylight simulation through Climatic-based metrics evaluation for West façade with thickness of 15 cm, West Façade.

Islamic Geometric Patterns	Daylight Autonomy			Useful Daylight illuminance			Exceeded Useful Daylight illuminance			sDA
	Bright	Semi-dark	Dark	Bright	Semi-dark	Dark	Bright	Semi-dark	Dark	
Base Model	89.25	72.3	57.65	31.96	64.65	68.75	60.18	23	0	100
8-Fold-Rosette	2.78	0.75	0.55	20.07	10.97	8.28	0.30	0.15	0	0
10-Fold-Rosette	0.25	0.25	0.32	1.77	0.05	0.04	0	0.06	0.05	0
Octagon	0.34	0.09	0.12	2.18	0	0	0	0	0	0
8-Point-Star	46.75	17.43	2	85.27	44.16	20.07	5.09	1.75	0.07	14.42
6-Point-Star	1.84	1.03	0.35	17.71	1.15	1.53	0.31	0.28	0	0

**Fig. 13.** Daylight glare probability of Orosi geometric patterns with thickness of 10 cm at Solstice and Equinox days during office hours, West façade.

4.2. Annual climate-based metrics and luminance-based metric of geometric patterns on the West Façade

4.2.1. Climate-based metrics evaluation for cases with thickness of 5 cm on West Façade

The results show the efficient role of the employed IGP in the Western façade for improving visual comfort. Table 7 confirmed that a thickness of 5 cm decreased the DA value in the bright layer (62.21%), which is the lowest value in comparison with the base model (99.56%) (Fig. 6(f)). Moreover, the semi-dark and dark layers experienced the lowest rate of 23.84% and 3.00% by Octagon (Fig. 6(b)). Based on Table n, the DA was significantly decreased. The UDI values of 88.64% (Octagon, Fig. 6(b)) in the bright layer and 93.24% (10-Fold-Rosette, Fig. 6(d)) in the semi-dark layers confirm the efficient performance of IGP in comparison with the base model (Fig. 6(f)). However, in the dark layer, all patterns showed a lower efficiency compared to the base model (Fig. 6(f)). Furthermore, the EUDI was significantly improved by the Octagon (Fig. 6(b)) in the bright layer (a reduction of 34.75%). Besides, the bar chart for the DGP values of 54 conducted simulations (Fig. 12) revealed that all the IGP simulations are in the imperceptible and perceptible range. The exceptions are observed only at 15:00 on 21st March and 21st June. The 8 Point-Star (Fig. 6(c)) and 8-Point-Star (Fig. 6(c)) brought

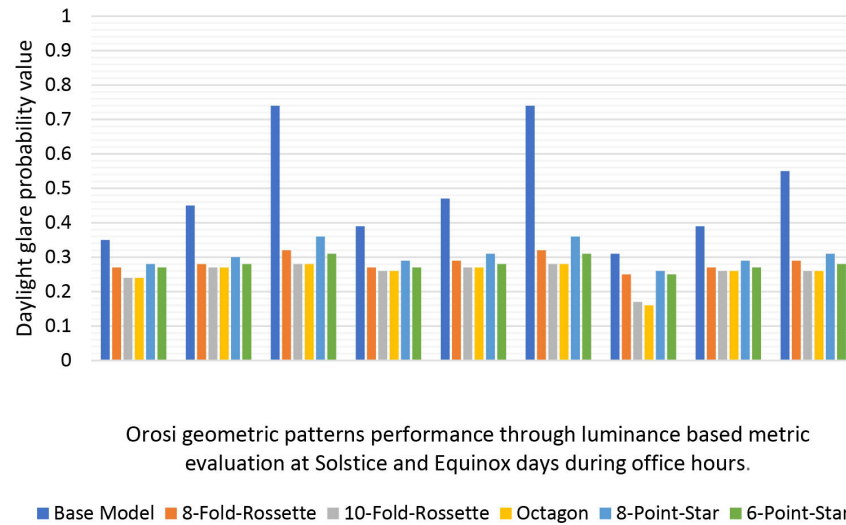
about a DGP value of more than 0.40 %, resulting in disturbing glare.

4.2.2. Climate-based metrics evaluation for cases with thickness of 10 cm, West Façade

Table 8 confirms the effectiveness of employing IGP in the Western façade to enhance the daylight condition and visual comforts. The results disclose a reduction in the DA values in all three layers. In this case, the maximum decline was achieved by 10-Fold-Rosette (Fig. 6(d)) in the bright layer and Octagon (Fig. 6(b)) in the semi-dark and dark layers. However, the DA value was improved to a satisfactory level, and the results point to the considerable decrease in UDI values, specifically in the semi-dark and dark layers by 10-Fold-Rosette (Fig. 6(d)) and Octagon (Fig. 6(b)), respectively. Moreover, comparing the EUDI values of the base model and IGP is indicative of a significant decrease. The maximum reduction in UDI occurred in the bright layer, experiencing a decrease from 42.78% to 1.25% (base model (Fig. 6(f)), Octagon (Fig. 6(b)), respectively). Moreover, to predict the risk of glare, a total of 54 simulations was conducted at three different times of the day (shown in Fig. 13). Despite the decrease in the DGP values compared to the base case, most of the results for the considered IGP were within the imperceptible and perceptible glare range. The results suggest that the glare requirements are met without any particular problems.

Table 9. Annual daylight simulation through Climatic-based metrics evaluation for West façade with thickness of 10 cm, West Façade.

Islamic Geometric Patterns	Daylight Autonomy			Useful Daylight illuminance			Exceeded Useful Daylight illuminance			sDA
	Bright	Semi-dark	Dark	Bright	Semi-dark	Dark	Bright	Semi-dark	Dark	
Base Model	89.25	72.3	57.65	31.96	64.65	68.75	60.18	23	0	100
8-Fold-Rosette	2.78	0.75	0.55	20.07	10.97	8.28	0.30	0.15	0	0
10-Fold-Rosette	0.25	0.25	0.32	1.77	0.05	0.04	0	0.06	0.05	0
Octagon	0.34	0.09	0.12	2.18	0	0	0	0	0	0
8-Point-Star	46.75	17.43	2	85.27	44.16	20.07	5.09	1.75	0.07	14.42
6-Point-Star	1.84	1.03	0.35	17.71	1.15	1.53	0.31	0.28	0	0

**Fig. 14.** Daylight glare probability of Orsi geometric patterns with thickness of 15 cm at Solstice and Equinox days during office hours, West Façade.

4.2.3. Climate-based metrics evaluation for cases with thickness of 15 cm, West Façade

Table 9 gives information about the effect of using IGPs in the Western façade. The 10-Fold-Rosette (Fig. 6(d)) decreased the DA value at the rate of 0.25% in the bright layer. Moreover, Octagon (Fig. 6(b)) achieved significant reductions down to the rate of 0.09% and 0.12% in the semi-dark and dark layers in comparison with the base model (99.56% (bright layer), 99.78% (semi-dark layer), and 75.67% (dark layer)). Moreover, a significant decrease was observed in the UDI values. The maximum reduction was down to the rate of 1.77% in the bright layer and 0.00% in the semi-dark and dark layers by 10-Fold-Rosette (Fig. 6(d)) and Octagon (Fig. 6(b)). Comparing Exceed UDI values for plain window and IGPs showed a significant decrease in from 42.78% to 0.00% in the bright layer by 10-Fold-Rosette (Fig. 6(d)) and Octagon (Fig. 6(b)). Moreover, the bar chart (Fig. 14) illustrates the DGP results for a total of 54 simulations in three different times of the day. The results confirm an improvement for all values, such that they remain within the imperceptible and perceptible range.

4.2.4. Differences between cases with thicknesses of 5, 10, and 15 cm on the West Façade

The findings confirmed the daylight performance of patterns with the 5 (Tables A.5 and A.7), 10 (Tables A.7 and A.8), and 15 cm (Tables A.9 and A.10) thickness on the West façade. In most of

the simulations, the indices were not observed within the appropriate ranges, specifically the sDA in thicknesses of 10 and 15 cm. The poor performance of patterns in providing DA, UDI, and Exceed UDI in both thicknesses resulted in an sDA value of 0.00% (by the 6-Point-Star (Fig. 6(a)), 10-Fold-Rosette (Fig. 6(d)), 8-Fold-Rosette (Fig. 6(e)), and Octagon (Fig. 6(b))) (Tables 4-6 and Figs. 12-14). IGPs with a thickness of 5 cm employed on the West facade showed a higher performance as shown in the following:

Use of the Octagon (Fig. 6(b)) and 10-Fold-Rosette (Fig. 6(d)) resulted in a minimum DA in all three layers. Although these patterns achieved high UDI values, their performances were not as expected in comparison to other patterns. In addition, both maintained the lowest rates of EUDI and DGP. Overall, with regards to the sDA values (25.96% and 25.00%, respectively), the Octagon and 10-Fold-Rosette failed to meet the required daylighting metrics within the adequate range.

The 6-Point-Star (Fig. 6(a)) achieved a considerable reduction in the rate of DA. Offering high UDI values of 87.59%, 88.25% and 42.12% (bright, semi-dark, and dark layer, respectively) approved the effective daylight performance. Additionally, the EUDI experienced a slight reduction through different layers. The DGP values were found in the imperceptible and perceptible range in all the situations. Overall, with regards to the sDA value (34.96%), the 6-Point-Star failed to meet the required daylighting metrics within the adequate range.

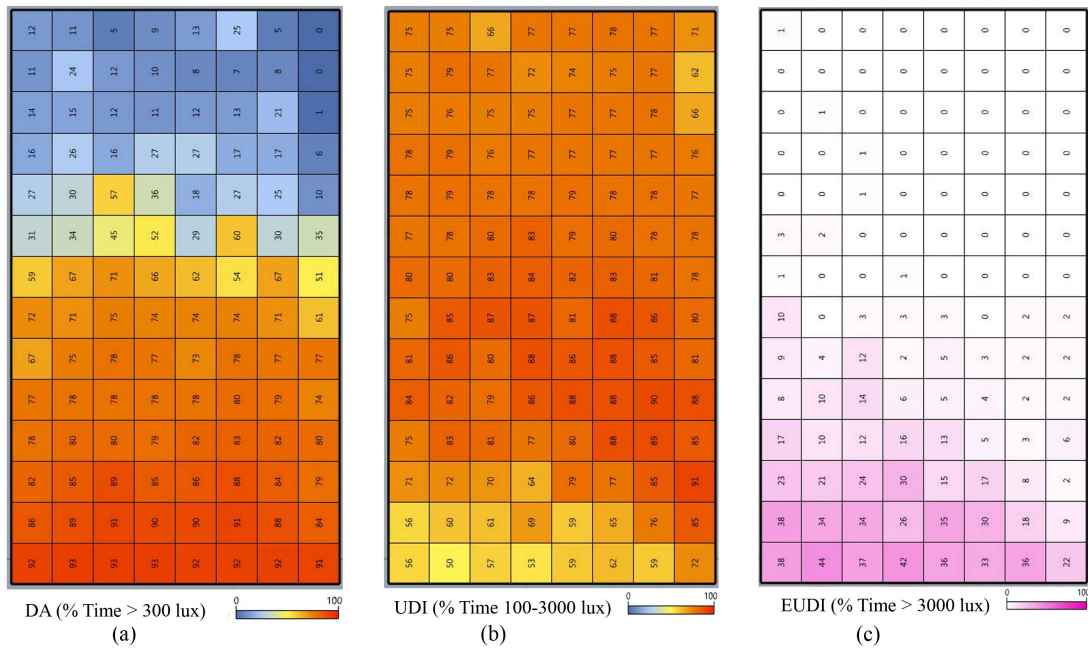


Fig. 15. Climate based daylight metrics grid evaluation (annual simulation) of 8-Point-Star for west facade (Fig. 5(c)). (a) Daylight Autonomy, (b) Useful Daylight illuminance, and (c) Exceed Useful Daylight illuminance.

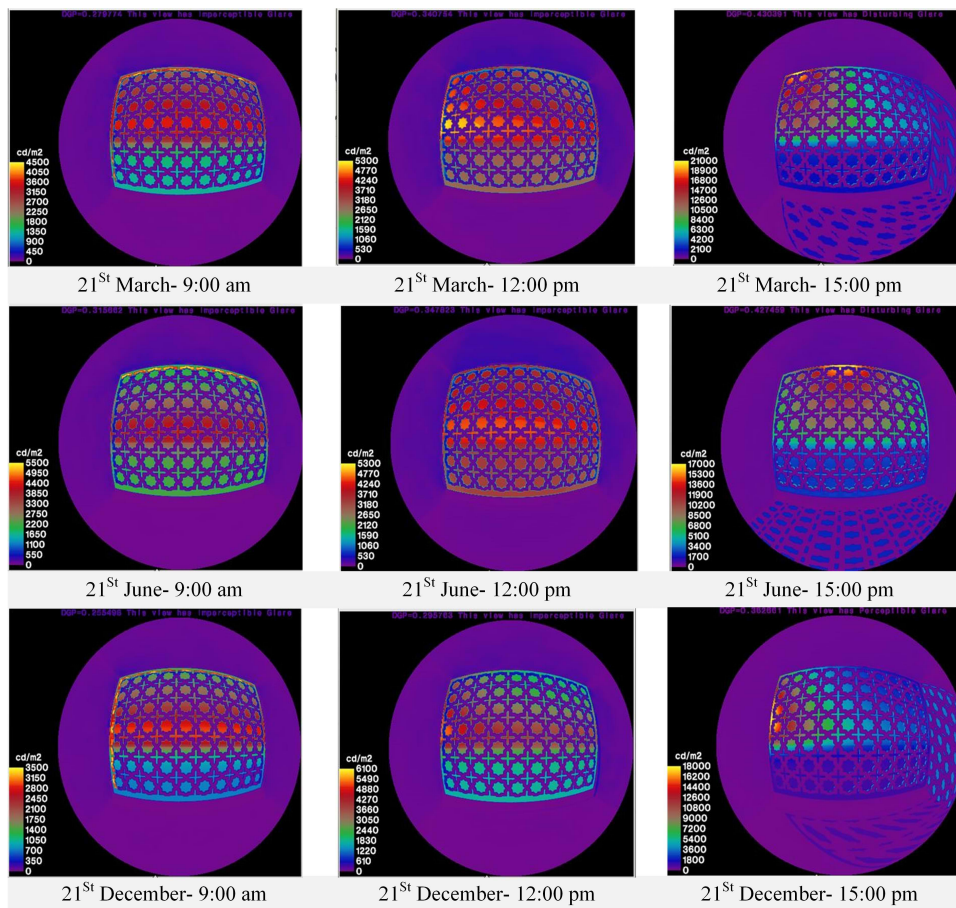


Fig. 16. Daylight glare probability (DGP) in three different days of 8-point-star for west facade (Fig. 5(c)).

The next pattern, 8-Fold-Rosette (Fig. 6(e)), decreased the amount of DA, especially in the semi-dark and dark layers. In the bright layer, a slight reduction was reported compared to the base model (94.28%, 99.56%, respectively). For the UDI, this pattern

provided the highest rates at semi-dark and dark layers (93.24%, 86.74%, respectively). Additionally, the low value of EUDI in the semi-dark (3.75%) and dark layers (0.07%) confirmed the effective performance of this pattern. Overall, with regards to the

sDA value (45.15%), the 8-Fold-Rosette was able to meet the required daylighting metrics within the adequate range.

The 8-Point-Star (Fig. 6(c)), as the last pattern, provided higher DA values, especially in the bright and dark layers. Additionally, it obtained high a UDI value, specifically in the semi-dark layer at a rate of 91.71%. The EUDI values were slightly improved using this pattern. Furthermore, the reduced DGP met the requirements of the imperceptible and the perceptible range. Exceptionally, a disturbing value was reported at 15:00 pm on 21st June and March. Overall, with regards to the sDA value (46.15%), the 8-Point-Star can meet the expectations of daylighting metrics to be within the adequate range.

5. Results and discussion

This study reveals the effectiveness of different Islamic Geometric Patterns applied in Orosies to improve indoor daylighting and visual comfort of occupants. Overall, all the patterns remarkably affect climate-based daylight metrics and luminance-based metric. However, since the impacts of different geometric patterns are different depending on their individual indicators, an accurate understanding of the simulation's feedback is contingent upon analyzing the results.

According to Tables 4-6 and Figs. 7-9 in the South façade, all the patterns kept DA within an adequate range for occupants. However, a thickness of 10 cm allowed a larger amount of daylight to enter, providing a higher portion of useful daylight for indoor space. For example, the 8-Point-Star (as the most appropriate pattern for the South façade) provided a DA value of 84.75% and 81.09% (for thicknesses of 10 cm and 15 cm, respectively) in the bright layer, which is more than twice the UDI value provided by the base model. Additionally, the patterns with a thickness of 15 cm offered a more effective performance in decreasing EUDI, consequently preventing thermal discomfort. For instance, 8-Point-Star achieved an average of EUDI value of 4.84% and 8.10 % for the 10 and 15 cm thicknesses, respectively, while the average UDI by the base model was 27.72%. Moreover, applying IGPs in the South façade decreased the DGP to the perceptible and imperceptible range in most of the situations. For example, 10-Fold-Rosette and Octagon significantly decreased the DGP from 0.74 to 0.29 (thickness of 10 cm) and 0.27 (thickness of 15 cm) at 9:00 on 21st March. Overall, based on daylight simulation, the 8-Point-Star pattern (Fig. 5(c)) with the 10 cm thickness achieved better results and fulfilled the daylight performance expectations. The 8-Point-Star proved its potential to improve daylight performance by offering an adequate DA value and controlling the UDI, Exceed UDI and sDA (45.50%). In terms of DGP, this prevented thermal discomfort in most of the scheduled time.

According to Tables 7-9 and Figs. 12-14, on the West façade, the indices were out of the appropriate ranges, specifically the sDA in thicknesses of 10 and 15 cm. The poor performance of patterns in the DA, UDI, and Exceed UDI indices in both thicknesses resulted in a 0.00% sDA (by the 6-Point-Star (Fig. 6(a)), 10-Fold-Rosette (Fig. 6(d)), 8-Fold-Rosette (Fig. 6(e)), and Octagon (Fig. 6(b))). IGPs with a thickness of 5 cm employed on the west faced offered better performance as they allowed more daylight to enter, providing the adequate range for occupants. In the case of UDI, these patterns provided high rates of useful daylight for indoor space. For example, the highest rates were achieved by 8-Fold-Rosette (Fig. 6(e)) at semi-dark and dark

layers (93.24%), while the base model offered a UDI of 88.06%. Moreover, the EUDI value was similar for all cases with only slight changes. For instance, Octagon decreased EUDI from 11.90% to 2.15% in the semi-dark layer and 1.55% to 0.05%. Nevertheless, the effect of each pattern varies in different hours of the day and different days of the month. The applied patterns decreased DGP, bringing it down to the acceptable range for occupants in most situations (Figs. 9 and 10). Overall, based on the findings, the 8-Point-Star pattern and 8-Fold-Rosette with the 5 cm thickness achieved better results and fulfilled the expectations. Bringing adequate DA amount, controlling UDI, and Exceed UDI and sDA (46.15% and 45.15%, 8-Point-Star, 8-Fold-Rosette, respectively) confirmed their potential in the improvement of daylight performance. In terms of DGP, these patterns prevented thermal discomfort due to solar heat gain in most of the scheduled timetable.

The comprehensive analysis of indexes gives an in-depth perspective about the advantages and disadvantages of each ornament, emphasizing the results can be employed in practical cases and designs. Hosseini et al. [25] evaluated the daylight performance of colored glass derived from Orosi at the south window in the hot and desert climate. According to the climate-based calculations, blue was the best choice for the bright layer that could meet all of the basic daylight requirements (DA: 52%, UDI: 74.67%, EUDI: 16.38), red the best choice for the semi-dark layer (DA: 36.39%, UDI: 87.33%, EUDI: 4%), and yellow or colorless the best choice for the dark layer (DA: 56.94%, UDI: 92.94%, EUDI: 0.00%). Among the geometric patterns, 8-point-Star obtained the average DA (43.39%), UDI (72.24%), and EUDI (4.84%) and provided sufficient and optimal daylight illuminance in the South orientation. It seems that the idea of combining different IGPs with colorful glasses might improve the IGP's daylight performance. The color can cover the poor daylight performance of IGPs and vice versa. For example, all of the patterns have approximately met imperceptible and perceptible rate for glare on 21st December, while daylight glare probability during office time for colorful glasses was disturbing with intolerable values. The combination of IGP and colorful glasses seems to have the potential to meet DGP visual requirements. This notion assists designers to appreciate the user preferences in selecting IGPs. Additionally, selecting appropriate color and pattern highly depends on the space function, local climate and user preferences.

6. Conclusion

In summary, this research investigates Islamic Geometric Patterns (IGPs) from the perspective of visual comfort and indoor daylight conditions intending to find appropriate patterns for daylight control in different orientations. The following questions were raised in this process: which IGPs have been employed in the Iranian Orosi windows? What are the IGPs' daylight functions and their differences in improving visual comfort of occupants? How the thickness of IGPs affect daylight performance? To find the answer to these questions, this study deeply explored Orosi windows in Iranian vernacular buildings. Based on the literature review, different functions have been identified, including decorative, thermal, and daylight roles. Additionally, a total of twelve traditional courtyard houses was studied through field survey to recognize different classes of IGPs used in the Orosies.

The following patterns were derived from the field survey: 6-Point-Star, Octagon, 8-Point-Star, 10-Fold-Rosette, and 8-Fold-Rosette. Subsequently, the daylight performance of the IGPs was evaluated in the Western and Southern facades at thicknesses of 5, 10, and 15 cm. The findings confirmed the high daylight performance of the IGPs and the positive effect of the thickness (5, 10, and 15 cm) in improving indoor daylight conditions and occupants' visual comfort. However, the efficiency of each pattern is different with respect to each individual indicator. Without geometric patterns, the windows allowed light to enter the room as much as possible. Using IGPs in the façade brings the opportunity of controlling how deep daylight penetrates space. For example, the 8-Point-Star, as the most appropriate pattern for the South façade provided DA, UDI, EUDI, and sDA values of 80.18%, 76.65%, 12.22%, 44.6 respectively for thicknesses of 10 cm in the bright layer, which is more than twice the UDI value provided by the base model. The comprehensive analysis of indexes gives an in-depth perspective of the advantages and disadvantages of each ornament, emphasizing the practical applications of the results in design and real-world scenarios. However, the simulation results were bound to a number of limitations and parameters that could affect them, specifically the

geometry of patterns. In fact, the appropriate patterns have been extracted based on the limited vernacular houses of Iran that could vary in different locations and climates. In particular, several types of patterns could have different effects on climate-based daylight metrics. Furthermore, a combination of geometric patterns and colors affects the amount of admitted daylight. Therefore, exploring a combination of IGPs and colored glass, different distribution patterns, and their impact on the users' preferences based on the space function can be the new topics for further research. Given that the present study evaluated the daylight performance of IGPs in a hot desert, future studies can conduct their simulation for other local climates. The editable and parametric geometries that generate different configurations can be investigated as a further research as well. Moreover, occupants' preferences for IGPs can be considered through a questionnaire survey. A real-test room can provide the opportunity to investigate the effectiveness of IGPs in comparison with the simulation results. IGPs can also be combined with kinetic façade as an active and innovative strategy to provide a real-time responsive façade in order to meet the visual comfort of the occupant.

Appendix A

Table A.1. Comparison patterns performance in terms of DA, UDI, EUDI, sDA values in thickness of 10cm, South Façade.

Metrics	Information
DA	Bright layer: Octagon < 10-Fold-Rosette < 6-Point-Star < 8-Fold-Rosette < 8-Point-Star < Base Model Semi-Dark Layer: Octagon < 10-Fold-Rosette < 6-Point-Star < 8-Fold-Rosette < 8-Point-Star < Base Model Dark Layer: 10-Fold-Rosette, Octagon < 6-Point-Star < 8-Point-Star < 8-Fold-Rosette < Base Model
UDI	Bright layer: Base Model < 8-Point-Star < Octagon < 10-Fold-Rosette < 8-Fold-Rosette < 6-Point-Star Semi-Dark Layer: Octagon < 10-Fold-Rosette < Base Model < 6-Point-Star < 8-Point-Star < 8-Fold-Rosette Dark Layer: Octagon < 10-Fold-Rosette < 6-Point-Star < 8-Point-Star < Base Model < 8-Fold-Rosette
EUDI	Bright layer: Octagon < 10-Fold-Rosette < 6-Point-Star < 8-Fold-Rosette < 8-Point-Star < Base Model Semi-Dark Layer: Octagon < 10-Fold-Rosette < 8-Fold-Rosette < 6-Point-Star < 8-Point-Star < Base Model Dark Layer: Octagon = 10-Fold-Rosette = 8-Fold-Rosette = 6-Point-Star = 8-Point-Star = Base Model
sDA	Octagon < 10-Fold-Rosette < 6-Point-Star < 8-Fold-Rosette < 8-Point-Star < Base Model

Table A.2. Comparison patterns performance in terms of DGP values in thickness of 10cm, South Façade.

Metrics	Information
21 st March	9:00 am: Octagon, 10-Fold-Rosette < 6-Point-Star < 8-Fold-Rosette < 8-Point-Star < Base Model 12:00 pm: Octagon, 10-Fold-Rosette < 6-Point-Star < 8-Fold-Rosette < 8-Point-Star < Base Model 15:00 pm: Octagon, 10-Fold-Rosette < 6-Point-Star < 8-Fold-Rosette < 8-Point-Star < Base Model
21 st June	9:00 am: Octagon, 10-Fold-Rosette < 6-Point-Star < 8-Fold-Rosette < 8-Point-Star < Base Model 12:00 pm: Octagon, 10-Fold-Rosette < 6-Point-Star < 8-Fold-Rosette < 8-Point-Star < Base Model 15:00 pm: Octagon < 10-Fold-Rosette < 6-Point-Star < 8-Fold-Rosette < 8-Point-Star < Base Model
21 st December	9:00 am: Octagon, 10-Fold-Rosette < 6-Point-Star, 8-Fold-Rosette, 8-Point-Star < Base Model 12:00 pm: Octagon, 10-Fold-Rosette < 6-Point-Star < 8-Fold-Rosette, 8-Point-Star < Base Model 15:00 pm: Octagon, 10-Fold-Rosette < 6-Point-Star, 8-Fold-Rosette < 8-Point-Star < Base Model

Table A.3. Comparison patterns performance in terms of DA, UDI, EUDI, sDA values in thickness of 15cm, South Façade.

Metrics	Information
DA	Bright layer: 10-Fold-Rosette < Octagon < 8-Fold-Rosette < 6-Point-Star < 8-Point-Star < Base Model Semi-Dark Layer: Octagon, 10-Fold-Rosette < 8-Fold-Rosette < 6-Point-Star < 8-Point-Star < Base Model Dark Layer: 10-Fold-Rosette, Octagon < 8-Fold-Rosette < 6-Point-Star < 8-Point-Star < Base Model
UDI	Bright layer: Base Model < 10-Fold-Rosette < Octagon < 8-Fold-Rosette < 8-Point-Star < 6-Point-Star Semi-Dark Layer: Octagon < 10-Fold-Rosette < 8-Fold-Rosette < Base Model < 6-Point-Star < 8-Point-Star Dark Layer: Octagon < 10-Fold-Rosette < 8-Fold-Rosette < 6-Point-Star < 8-Point-Star < Base Model
EUDI	Bright layer: 10-Fold-Rosette, Octagon < 8-Fold-Rosette < 6-Point-Star < 8-Point-Star < Base Model Semi-Dark Layer: 10-Fold-Rosette, Octagon < 8-Fold-Rosette < 8-Point-Star < 6-Point-Star < Base Model Dark Layer: Octagon = 10-Fold-Rosette = 8-Fold-Rosette = 6-Point-Star = 8-Point-Star = Base Model
sDA	Octagon, 10-Fold-Rosette, 8-Fold-Rosette < 6-Point-Star < 8-Point-Star < Base Model

Table A.4. comparison patterns performance in terms of DGP values in thickness of 15cm, South Façade.

Metrics	Information
21 st March	9:00 am: Octagon, 10-Fold-Rosette < 6-Point-Star, 8-Fold-Rosette < 8-Point-Star < Base Model
	12:00 pm: Octagon < 10-Fold-Rosette < 6-Point-Star < 8-Fold-Rosette < 8-Point-Star < Base Model
	15:00 pm: Octagon, 10-Fold-Rosette < 6-Point-Star < 8-Fold-Rosette < 8-Point-Star < Base Model
21 st June	9:00 am: Octagon < 10-Fold-Rosette, 6-Point-Star < 8-Fold-Rosette < 8-Point-Star < Base Model
	12:00 pm: Octagon, 10-Fold-Rosette < 6-Point-Star < 8-Fold-Rosette < 8-Point-Star < Base Model
	15:00 pm: Octagon, 10-Fold-Rosette < 6-Point-Star, 8-Fold-Rosette < 8-Point-Star < Base Model
21 st December	9:00 am: Octagon, 10-Fold-Rosette < 6-Point-Star, 8-Fold-Rosette < 8-Point-Star < Base Model
	12:00 pm: Octagon, 10-Fold-Rosette < 6-Point-Star < 8-Fold-Rosette < 8-Point-Star < Base Model
	15:00 pm: Octagon, 10-Fold-Rosette < 6-Point-Star, 8-Fold-Rosette < 8-Point-Star < Base Model

Table A.5. comparison patterns performance in terms of DA, UDI, EUDI, sDA values in thickness of 5 cm, West façade.

Metrics	Information
DA	Bright layer: 10-Fold-Rosette < Octagon < 6-Point-Star < 8-Fold-Rosette < 8-Point-Star < Base Model
	Semi-Dark Layer: Octagon < 10-Fold-Rosette < 6-Point-Star < 8-Fold-Rosette < 8-Point-Star < Base Model
	Dark Layer: Octagon < 10-Fold-Rosette < 6-Point-Star < 8-Point-Star < 8-Fold-Rosette < Base Model
UDI	Bright layer: Base Model < 8-Point-Star < 8-Fold-Rosette < 6-Point-Star < 10-Fold-Rosette < Octagon
	Semi-Dark Layer: Octagon < 10-Fold-Rosette < Base Model < 6-Point-Star < 8-Point-Star < 8-Fold-Rosette
	Dark Layer: Octagon < 10-Fold-Rosette < 6-Point-Star < 8-Point-Star < 8-Fold-Rosette < Base Model
EUDI	Bright layer: Octagon < 10-Fold-Rosette < 6-Point-Star < 8-Fold-Rosette < 8-Point-Star < Base Model
	Semi-Dark Layer: Octagon < 10-Fold-Rosette < 6-Point-Star < 8-Fold-Rosette < 8-Point-Star < Base Model
	Dark Layer: Octagon < 8-Fold-Rosette < 10-Fold-Rosette < 6-Point-Star < 8-Point-Star < Base Model
sDA	Octagon < 10-Fold-Rosette < 6-Point-Star < 8-Fold-Rosette < 8-Point-Star < Base Model

Table A.6. Comparison patterns performance in terms of DGP values in thickness of 5cm, West façade.

Metrics	Information
21 st March	9:00 am: Octagon, 10-Fold-Rosette, 8-Point-Star < 8-Fold-Rosette, 6-Point-Star < Base Model
	12:00 pm: Octagon, 10-Fold-Rosette < 6-Point-Star < 8-Fold-Rosette < 8-Point-Star < Base Model
	15:00 pm: Octagon, 10-Fold-Rosette < 6-Point-Star < 8-Point-Star < 8-Fold-Rosette < Base Model
21 st June	9:00 am: Octagon, 10-Fold-Rosette < 6-Point-Star < 8-Fold-Rosette, 8-Point-Star < Base Model
	12:00 pm: Octagon, 10-Fold-Rosette < 6-Point-Star < 8-Fold-Rosette, 8-Point-Star < Base Model
	15:00 pm: Octagon, 10-Fold-Rosette < 6-Point-Star < 8-Point-Star < 8-Fold-Rosette < Base Model
21 st December	9:00 am: Octagon, 10-Fold-Rosette, 6-Point-Star < 8-Fold-Rosette, 8-Point-Star < Base Model
	12:00 pm: Octagon, 10-Fold-Rosette < 6-Point-Star < 8-Point-Star, 8-Fold-Rosette < Base Model
	15:00 pm: Octagon, 10-Fold-Rosette, 6-Point-Star < 8-Fold-Rosette, 8-Point-Star < Base Model

Table A.7. Comparison patterns performance in terms of DA, UDI, EUDI, and sDA values in thickness of 10cm, West Façade.

Metrics	Information
DA	Bright layer: 10-Fold-Rosette < Octagon < 6-Point-Star < 8-Fold-Rosette < 8-Point-Star < Base Model
	Semi-Dark Layer: Octagon < 10-Fold-Rosette < 6-Point-Star < 8-Fold-Rosette < 8-Point-Star < Base Model
	Dark Layer: Octagon < 10-Fold-Rosette < 6-Point-Star < 8-Fold-Rosette < 8-Point-Star < Base Model
UDI	Bright layer: 10-Fold-Rosette < Octagon < Base Model < 6-Point-Star < 8-Fold-Rosette < 8-Point-Star
	Semi-Dark Layer: 10-Fold-Rosette < Octagon < 6-Point-Star < 8-Fold-Rosette < 8-Point-Star < Base Model
	Dark Layer: Octagon < 10-Fold-Rosette < 6-Point-Star < 8-Fold-Rosette < 8-Point-Star < Base Model
EUDI	Bright layer: 10-Fold-Rosette < Octagon < 8-Fold-Rosette < 6-Point-Star < 8-Point-Star < Base Model
	Semi-Dark Layer: Octagon < 10-Fold-Rosette < 8-Fold-Rosette < 6-Point-Star < 8-Point-Star < Base Model
	Dark Layer: Octagon = 10-Fold-Rosette = 8-Fold-Rosette = 6-Point-Star < 8-Point-Star < Base Model
sDA	Octagon = 10-Fold-Rosette = 6-Point-Star < 8-Fold-Rosette < 8-Point-Star < Base Model

Table A.8. Comparison patterns performance in terms of DGP values in thickness of 10cm, West Façade.

Metrics	Information
21 st March	9:00 am: Octagon, 10-Fold-Rosette < 8-Fold-Rosette, 6-Point-Star < 8-Point-Star < Base Model
	12:00 pm: Octagon, 10-Fold-Rosette < 6-Point-Star < 8-Fold-Rosette < 8-Point-Star < Base Model
	15:00 pm: Octagon, 10-Fold-Rosette < 6-Point-Star < 8-Fold-Rosette < 8-Point-Star < Base Model
21 st June	9:00 am: Octagon, 10-Fold-Rosette < 6-Point-Star, 8-Fold-Rosette < 8-Point-Star < Base Model
	12:00 pm: Octagon, 10-Fold-Rosette < 6-Point-Star < 8-Fold-Rosette < 8-Point-Star < Base Model
	15:00 pm: Octagon, 10-Fold-Rosette < 6-Point-Star < 8-Fold-Rosette < 8-Point-Star < Base Model
21 st December	9:00 am: Octagon, 10-Fold-Rosette, 6-Point-Star, 8-Fold-Rosette, 8-Point-Star < Base Model

12:00 pm: Octagon < 6-Point-Star < 8-Fold-Rosette < 10-Fold-Rosette, 8-Point-Star < Base Model
 15:00 pm: Octagon, 10-Fold-Rosette < 6-Point-Star < 8-Fold-Rosette < 8-Point-Star < Base Model

Table A.9. Comparison patterns performance in terms of DA, UDI, EUDI, and sDA values in thickness of 15 cm, West Façade.

Metrics	Information
DA	Bright layer: 10-Fold-Rosette < Octagon < 6-Point-Star < 8-Fold-Rosette < 8-Point-Star < Base Model Semi-Dark Layer: Octagon < 10-Fold-Rosette < 8-Fold-Rosette < 6-Point-Star < 8-Point-Star < Base Model Dark Layer: Octagon < 10-Fold-Rosette < 6-Point-Star < 8-Fold-Rosette < 8-Point-Star < Base Model
UDI	Bright layer: 10-Fold-Rosette < Octagon < 6-Point-Star < 8-Fold-Rosette < Base Model < 8-Point-Star Semi-Dark Layer: Octagon < 10-Fold-Rosette < 6-Point-Star < 8-Fold-Rosette < 8-Point-Star < Base Model Dark Layer: Octagon < 10-Fold-Rosette < 6-Point-Star < 8-Fold-Rosette < 8-Point-Star < Base Model
EUDI	Bright layer: Octagon = 10-Fold-Rosette < 8-Fold-Rosette < 6-Point-Star < 8-Point-Star < Base Model Semi-Dark Layer: Octagon < 10-Fold-Rosette < 8-Fold-Rosette < 6-Point-Star < 8-Point-Star < Base Model Dark Layer: Octagon = 8-Fold-Rosette = 6-Point-Star < 10-Fold-Rosette < 8-Point-Star < Base Model
sDA	Octagon = 10-Fold-Rosette = 8-Fold-Rosette = 6-Point-Star < 8-Point-Star < Base Model

Table A.10. Comparison patterns performance in terms of DGP values in thickness of 15cm, West Façade.

Metrics	Information
21 st March	9:00 am: Octagon, 10-Fold-Rosette < 6-Point-Star, 8-Fold-Rosette < 8-Point-Star < Base Model 12:00 pm: Octagon, 10-Fold-Rosette < 6-Point-Star, 8-Fold-Rosette < 8-Point-Star < Base Model 15:00 pm: Octagon, 10-Fold-Rosette < 6-Point-Star < 8-Fold-Rosette < 8-Point-Star < Base Model
21 st June	9:00 am: Octagon, 10-Fold-Rosette < 6-Point-Star, 8-Fold-Rosette < 8-Point-Star < Base Model 12:00 pm: Octagon, 10-Fold-Rosette < 6-Point-Star < 8-Fold-Rosette < 8-Point-Star < Base Model 15:00 pm: Octagon, 10-Fold-Rosette < 6-Point-Star < 8-Fold-Rosette < 8-Point-Star < Base Model
21 st December	9:00 am: Octagon < 10-Fold-Rosette < 6-Point-Star, 8-Fold-Rosette < 8-Point-Star < Base Model 12:00 pm: Octagon, 10-Fold-Rosette < 6-Point-Star, 8-Fold-Rosette < 8-Point-Star < Base Model 15:00 pm: Octagon, 10-Fold-Rosette < 6-Point-Star < 8-Fold-Rosette < 8-Point-Star < Base Model

Contributions

S. N. Hosseini: Conceptualization, Methodology, Writing-original draft, Visualization, Investigation, Validation, Writing- review & editing. S. M. Hosseini: Supervision, Conceptualization, Methodology, Software, Data curation, Investigation, Validation, Writing- review & editing. M. HeiraniPour: Software, Data curation.

Declaration of competing interest

The authors report no conflicts of interest.

References

- [1] S. M. Hosseini, M. Mohammadi, and O. Guerra-Santin, Interactive kinetic façade: Improving visual comfort based on dynamic daylight and occupant's positions by 2D and 3D shape changes, *Building and Environment* 165 (2019) 106396.
- [2] R. Debnath and R. Bardhan, Daylight Performance of a Naturally Ventilated Building as Parameter for Energy Management, *Energy Procedia* 90 (2016) 382–394.
- [3] X. Yu and Y. Su, Daylight availability assessment and its potential energy saving estimation: A literature review, *Renewable and Sustainable Energy Reviews* 52 (2015) 494–503.
- [4] M. Tahbaz and F. Mousavi, Daylighting methods in iranian traditional architecture (green lighting), *Proceeding CISBAT, EPFL, Lausanne, Switzerland* (2009), 273–278. Available: https://www.academia.edu/6050383/Daylighting_Methods_in_Iranian_Traditional_Architecture_Green_Lighting.
- [5] E. Maghsoudi Nia, T. Hajihassani, M. Y. Mohd Yunos, and N. Abdul Rahman, Daylighting Strategies in Iranian Vernacular Residential Buildings in Hot and Dry Climate, *Applied Mechanics and Materials* 747 (2015) 329–332.
- [6] C. L. Robbins, *Daylighting: Design and analysis*, New York, N.Y., Van Nostrand Reinhold, 1986.
- [7] J. Mardaljevic, Daylight daylight/daylighting, *Indoor Illumination indoor illumination, and Human Behavior*, in *Encyclopedia of Sustainability Science and Technology*, New York, NY: Springer New York, 2012.
- [8] S. Chien and K. J. Tseng, Assessment of climate-based daylight performance in tropical office buildings: a case study, *International Journal of Low-Carbon Technologies* 9 (2014) 100–108.
- [9] S. Nazidizaji and H. Safari, The Social Logic of Persian Houses, in Search of the Introverted Houses Genotype, *World Applied Sciences Journal* 26, (2013) 817–825.
- [10] A. Zand Karimi and B. Hosseini, The Influence of Iranian Islamic Architecture on Traditional Houses of Kashan, In: *Archi-Cultural Translations through the Silk Road 2nd International Conference* (2012), Nishinomiya, Japan.
- [11] H. Aljawder and H. El-Wakeel, Privacy Vs. Daylight: Evaluating the Acceptance of Daylighting Traditional Devices in Contemporary Residential Houses in Bahrain, *International Journal of Sustainable Development and Planning* 15 (2020) 655–663.
- [12] S. M. Hosseini, M. Mohammadi, A. Rosemann, T. Schröder, and J. Lichtenberg, A morphological approach for kinetic façade design process to improve visual and thermal comfort: Review, *Building and Environment* 153 (2019) 186–204.
- [13] R. Hyde, *climate responsive design: a study of buildings in moderate and hot humid climates*, Taylor & Francis, 2013.
- [14] T. Dahl, *Climate and Architecture*. Milton Park, Abingdon, Oxon; New York, N.Y., 2010.
- [15] N. Hourigan, Confronting Classifications - When and What is Vernacular Architecture?, *Civil Engineering and Architecture* 3 (2015) 22–30.
- [16] F. B. M. Baboli, N. Ibrahim, and D. M. Sharif, Design Characteristics and Adaptive Role of the Traditional Courtyard Houses in the Moderate Climate of Iran, *Procedia - Social and Behavioral Sciences* 201 (2015) 213–223.
- [17] C. Morgan, R. De Dear, and G. Brager, Climate, clothing and adaptation in the built environment, in: *9th International Conference on Indoor Air Quality and Climate* (2002), 98–103. [Online]. Available: <http://www.irbdirekt.de/daten/iconda/CIB7766.pdf>.
- [18] M. Shabani, M. Tahir, A. Che-Ani, N. A. Abdullah, and I. M. Usman, Achieving privacy in the Iranian contemporary compact apartment through flexible design, *Selected Topics In Power Systems And Remote Sensing* (2010) 285–296. [Online]. Available: <https://www.semanticscholar.org/paper/Achieving-privacy-in-the-Iranian-contemporary-Shabani-Tahir/2d504f94e3d3578640b2b80e9594ff2efa4b0762>.
- [19] M. Kasmaei, *Climate and Architecture*. Isfahan: Nashr-e-Khak, 2003.

- [20] M. Tahbaz, S. Jalilian, F. Mousavi, and M. Kazemzadeh, Natural daylighting in traditional houses in kashan, case study of ameri house., Iranian architecture studies 4 (2014), 87–108. [Online]. Available: http://jias.kashanu.ac.ir/files/site1/user_files_dbc6fd/a_omrani-A-10-27-27-7abd13e.pdf.
- [21] H. Shahamat, Formal Sustainability in Traditional Architecture of Iran According To Five Principles of Traditional Architecture of Iran, Journal of applied environmental and biological sciences 4 (2014) 100–110.
- [22] F. Nabavi, Y. Ahmad, and A. T. Goh, Daylight Design Strategies: A Lesson from Iranian Traditional Houses, Mediterranean Journal of Social Sciences 9 (2013) 97-103.
- [23] F. Kateb, Window in Iran Islamic Architecture with Emphasis on Role of Light, Journal of History Culture and Art Research 7 (2018) 215.
- [24] P. Faghihi, F. Quintas, and T. Almeida, Architectural glass in the 18th to 20th centuries in Iran, In: Glass science in art Conservation, 2017, pp. 43–45.
- [25] S. M. Hosseini, M. Mohammadi, A. Rosemann, and T. Schröder, Quantitative Investigation Through Climate-based Daylight Metrics of Visual Comfort Due to Colorful Glass and Orosi Windows in Iranian Architecture, Journal of Daylighting 5 (2018) 21–33.
- [26] F. Habib, F. Alborzi, and I. Etesam, Light Processing in Iranian Houses; Manifestation of Meanings and Concepts, International Journal of Architecture and Urban Development 3 (2013), 11–20. [Online]. Available: http://ijaud.srbiau.ac.ir/article_1647.html.
- [27] F. Kateb, architecture of iranian houses. Tehran: Islamic guidance and culture publication, 2005.
- [28] H. Fathi and E. Zarei Farasani, comparative study of elements and proprieties in orsies of zand and qajar periods, Trends in Life Science 3 (2014).
- [29] M. MadhoushianNezhad and H. Askari Alamoti, Tabriz Qajar Sash, Qualitative and Quantitative Distinctions, Design and Role, Sash Making Techniques, Fine Arts Journal 21 (2016) 77–84.
- [30] A. Mofrad Boushehri and Y. Gorji Mahlabani, The Analysis of Daylight Factor and Illumination in Iranian Traditional Architecture, Case Studies: Qajar Era Houses, Qazvin, Arman Shahr 10 (2017), 35–45. [Online]. Available: http://www.armanshahrjournal.com/article_49201.html.
- [31] A. Khamechian, M. Azad, and M. Tahbaz, geometric analysis and proportions of orosi windows's case study: 7 orosi of kashan houses. Journal of iranian handicrafts, Journal of Iranian Handicrafts 1(2018) 5–23.
- [32] S. M. Hosseini, M. Mohammadi, T. Schröder, and O. Guerra-Santin, Integrating interactive kinetic façade design with colored glass to improve daylight performance based on occupants' position, Journal of Building Engineering 31 (2020) 101-404.
- [33] Y. Gorji Mahlabani and A. Mofrad Boushehri, Orosi, a Way to Control Daylight Case Studies: Qajar Period Houses in Qazvin, Journal of Iranian Architecture and Urbanism 7 (2017) 225-236.
- [34] M. Haghshenas, M. R. Bemanian, and Z. Ghiabaklou, Analysis the Criteria of Solar Transmittance from Stained Glasses Used in Some of the Orosis from Safavid Dynasty, Journal of Color Science and Technology 10 (2016) 55–64.
- [35] M. Wahdattalab and A. Nikmaram, An Investigation into the Importance, Abundance and Distribution of Red Color in Stained Glass Windows of Historical Houses in Iran Case Study: 22 Examples of Stained Glass Windows Circle Heads (Crowns) in Houses built during Qajar Dynasty in Tabriz, Journal of Fine Art 22 (2017) 87–97.
- [36] M. H. Vaafi, Windows in Residential Architecture of Safavid Period in Isfahan, Honar 52 (2002) 131–136.
- [37] M. Boubekri, Daylighting, Architecture and Health: Building Design Strategies, 1st Edition, Routledge, 2008.
- [38] S. Ayvazian, Light in Traditional and Islamic Architecture of Iran, Journal of Architecture and Urban Planning 5 (2004) 12–38.
- [39] H. R. Sharif, A. Habibi, and A. Jamalabadi, Climatic Function of Garih Art in Islamic Architecture, Case study: Residential building at Qajar Era in Shiraz, Journal of Researches in Islamic Architecture Iran University of Science and Technology 4 (2017) 60–71. [Online]. Available: <http://jria.iust.ac.ir/article-1-617-en.html>.
- [40] A. Javani, Z. Javani, and M. R. Mashkforoush, Studying Relationship Between Application of Light and Iranian Pattern of Thought (the Iranians Ideology), In: Colour and Light in Architecture First International Conference Proceedings (2010), Venice, Italy, 39–46. [Online]. Available: [http://archsabat.com/pdf/Studying_Relationship_Between_Applications_of_Light_and_the_Iranians_Pattern_of_Thought_\(the_Iranian_Ideology\)-Book-co_author-Italy.pdf](http://archsabat.com/pdf/Studying_Relationship_Between_Applications_of_Light_and_the_Iranians_Pattern_of_Thought_(the_Iranian_Ideology)-Book-co_author-Italy.pdf).
- [41] T. Jalili and L. Nazari Poorgol Sefidi, the Survey of the Color and Light Psychological Effects in Iranian Traditional Architecture (Case Study: Tabataba'ees House), Iioab Journal 7 (2016) 469–483.
- [42] M. MadhoushianNezhad and H. Askari Alamoti, Qualitative and Quantitative Differentiation, Pattern and Construction Techniques of Qajarian Orosies in Tabriz, Fine Arts Journal 21 (2016) 77–84.
- [43] Y. Abdullahi and M. R. Bin Embi, Evolution of Islamic Geometric Patterns, Frontiers of Architectural Research 2 (2013) 243–251.
- [44] A. Marotta, Technologies to Know and Share the Cultural Heritage Between East and West: Geometric Patterns in the Decorations, In Le Vie dei Mercanti XIII Forum Internazionale di Studi (2015), Italy, 1353–1362. [Online]. Available: <https://core.ac.uk/download/pdf/76530693.pdf>.
- [45] M. Tahbaz, F. Mousavi, and S. Jalilian, Door Window Daylighting Evaluation in Traditional Houses of Iran, In International Conference of CISBAT 1 (2013), Switzerland.
- [46] M. Tahbaz, F. Mousavi, and S. Jalilian, Assessment of Iranian Traditional Door-Windows A Proposal to Improve Daylighting System in Classrooms, Fine Arts Journal 8 (2011).
- [47] M. Kazemzadeh and M. Tahbaz, Measurement and Analyzing Daylight Condition in Traditional Kerman Houses (Aminian House), Fine Arts Journal 18 (2013) 17–26.
- [48] F. Mousavi, M. Mahmodi, and M. Tahbaz, The Effect of Geometry and Area of Windows of Southview Rooms on The Depth of Daylighting Case Study: Yazd's Traditional Houses, Hoviatshahr 12 (2019), 5–18. Available: http://hoviatshahr.srbiau.ac.ir/article_13915_en.html.
- [49] V. Makani, A. Khorram, and Z. Ahmadipour, Secrets of Light in Traditional Houses of Iran, International Journal of Architecture and Urban Development 2 (2012) 45–50. Available: http://journals.srbiau.ac.ir/article_570.html.
- [50] S. Manoukian, City of Knowledge in Twentieth Century Iran: Shiraz, History and Poetry. Routledge, 2012.
- [51] A. Assari and T. M. Mahesh, Demographic Comparative in Heritage Texture of Isfahan City, Journal of Geography and Regional Planning 4 (2011) 463–470. Available: https://academicjournals.org/article/1381844733_Assari_and_Mahesh.pdf.
- [52] J.M. Jafari, History of Yazd. Tehran, Iran: Scientific and Cultural Publishing Company, 1964.
- [53] K. HajiGhasemi, Ganjnameh: Cyclopaedia of Iranian Islamic Architecture: 3. Spiritual Buildings of Tehran. Tehran, Iran: Shashid Beheshti Uniersity, Faculty of Architecture and Urban Planning, 1998.
- [54] H. Koliji, Gazing Geometries: Modes of Design Thinking in Pre-Modern Central Asia and Persian Architecture, Nexus Network Journal 18 (2016) 105–132.
- [55] A. S. Ahmed, The Spiritual Search of Art Over Islamic Architecture with Non-Figurative Representations, Journal of Islamic Architecture 3 (2014) 1-13.
- [56] S. Cenani and G. Cagdas, A Shape Grammar Study: Form Generation with Geometric Islamic Patterns, In Proceedings of the 24th Ecaade (2006), pp. 292.
- [57] M. Meraji, Arg of KarimKhan, Wikimedia Commons (2017).
- [58] A. EbrahimZadeh, Kianpour (Gilanian) House in Isfahan, SAJ Wood Craft (2019). Available: <http://sajwood.com/خانهکیانپورگیلانیان-اصفهان/>.
- [59] A. EbrahimZadeh, House and Museum of Lariha in Yazd, SAJ Wood Craft (2019). Available: <http://sajwood.com/خانهموزه-لاری-ها/>.
- [60] C. Reinhart, Daylight performance predictions. In: Building Performance Simulation for Design and Operation, 2nd Edition, London: Routledge 792 (2019) 221-269.
- [61] C. Reinhart, Daylight performance predictions, Building Performance Simulation for Design and Operation. Spon Press, 2011.
- [62] J. Wienold and J. Christoffersen, Evaluation methods and development of a new glare prediction model for daylight environments with the use of CCD cameras, Energy and Buildings 38 (2006) 743–757.
- [63] D. Chen and H. W. Chen, Using the Köppen Classification to Quantify Climate Variation and Change: an Example for 1901–2010, Environmental Development 6 (2013) 69–79.
- [64] National Renewable Energy Laboratory. Weather Data by Location, Asia WMO Region 2 - Iran - Islamic Republic of [Internet]. EnergyPlus. 2019 [cited 2019 Apr 16]. Available: https://energyplus.net/weather-location/asia_wmo_region_2/IRN/IRN_Yazd.408210_ITMY.